GTPase cross talk regulates TRAPPII activation of Rab11 homologues during vesicle biogenesis

Laura L. Thomas and J. Christopher Fromme

Department of Molecular Biology and Genetics, Weill Institute for Cell and Molecular Biology, Cornell University, Ithaca, NY 14853

Rab guanosine triphosphatases (GTPases) control cellular trafficking pathways by regulating vesicle formation, transport, and tethering. Rab11 and its paralogs regulate multiple secretory and endocytic recycling pathways, yet the guanine nucleotide exchange factor (GEF) that activates Rab11 in most eukaryotic cells is unresolved. The large multisubunit transport protein particle (TRAPP) II complex has been proposed to act as a GEF for Rab11 based on genetic evidence, but conflicting biochemical experiments have created uncertainty regarding Rab11 activation. Using physiological Rab-GEF reconstitution reactions, we now provide definitive evidence that TRAPPII is a bona fide GEF for the yeast Rab11 homologues Ypt31/32. We also uncover a direct role for Arf1, a distinct GTPase, in recruiting TRAPPII to anionic membranes. Given the known role of Ypt31/32 in stimulating activation of Arf1, a bidirectional cross talk mechanism appears to drive biogenesis of secretory and endocytic recycling vesicles. By coordinating simultaneous activation of two essential GTPase pathways, this mechanism ensures recruitment of the complete set of effectors needed for vesicle formation, transport, and tethering.

Introduction

A major challenge for eukaryotic cells is the need to transport cargo between membrane-bound organelles in a regulated manner. Virtually every step of trafficking is coordinated by Rab GTPases, which recruit effectors that facilitate vesicle budding, transport, tethering, and fusion (Cai et al., 2007; Barr, 2009; Glick and Nakano, 2009; Pfeffer, 2012; Novick, 2016). Rab GTPase function itself is controlled by guanine nucleotide exchange factors (GEFs), which catalyze nucleotide exchange to convert inactive GDP-bound Rabs to their active GTP-bound state, in which they are anchored to membranes through C-terminal prenyl modifications.

In yeast, the Rab GTPases Ypt1 and Ypt31/32 regulate entry to and exit from the Golgi complex, respectively, and thus are of critical importance to the secretory pathway (Segev, 2001). Ypt1 (Rab1) functions on ER-derived COPII vesicles and the Golgi to regulate several membrane sorting steps, including ER-to-Golgi trafficking, endocytic recycling, and autophagosome formation (Jedd et al., 1995; Lynch-Day et al., 2010; Sclafani et al., 2010). Ypt31/32 (Rab11) facilitates the formation of vesicles at the trans-Golgi network (TGN) and the subsequent transport and docking of these vesicles at the plasma membrane (Benli et al., 1996; Jedd et al., 1997; Mizuno-Yamasaki et al., 2010; Santiago-Tirado et al., 2011). Vesicle biogenesis at the TGN depends on the Arf-GEF Sec7, which activates the GTPase Arf1 to recruit cargo adaptors, coat proteins, and lipid-modifying enzymes (Jackson and Bouvet, 2014). Recent work has identified Ypt31/32 as a major regulator of Sec7 activity (McDonold and Fromme, 2014), establishing the role of Ypt31/32 as a key driver of vesicle formation at the TGN.

Despite the significance of Ypt1 and Ypt31/32 as essential regulators of the secretory pathway, the identities of the GEFs that activate Ypt1 and Ypt31/32 remain controversial. Several studies implicate the transport protein particle (TRAPP) complex family as GEFs for both Ypt1 and Ypt31/32 (Jones et al., 2000; Wang et al., 2000; Morozova et al., 2006). Current models describe two TRAPP complexes that regulate the secretory pathway in yeast: TRAPPI is implicated in ER-to-Golgi transport, and TRAPPII is proposed to facilitate intra-Golgi transport, secretory vesicle formation, and endosome recycling (Barrowman et al., 2010; Brunet and Sacher, 2014). Both complexes share seven core subunits, whereas TRAPPII is distinguished by the inclusion of four additional complex-specific subunits (Fig. 1 A).

Several lines of genetic evidence suggest that TRAPPII is a Ypt31/32 GEF (Yamamoto and Jigami, 2002; Zhang et al., 2002; Sciorra et al., 2005; Morozova et al., 2006), and TRAPPII has been shown to function upstream of Ypt31/32 homologues in *Aspergillus nidulans* as well as in mammalian, plant, and insect cells (Robinett et al., 2009; Qi et al., 2011; Westlake et al.,

Correspondence to J. Christopher Fromme: jcf14@cornell.edu

Abbreviations used: BFA, brefeldin A; BME, β-mercaptoethanol; CI, confidence interval; DOPC, dioleoylphosphatidylcholine; GDI, GDP dissociation inhibitor; GEF, guanine nucleotide exchange factor; GGPP, geranylgeranyl pyrophosphate; PC, phosphatidylcholine; PH, pleckstrin homology; PI, phosphatidylinositol; PI(4)P, phosphatidylinositol 4-phosphate; PS, phosphatidylserine; REP, Rab escort protein; rTRAPP, recombinant transport protein particle; TAP, tandem affinity purification; TB, Terrific Broth; TRAPP, transport protein particle; WT, wild-type.

The Rockefeller University Press $30.00
J. Cell Biol. Vol. 215 No. 4 499–513
https://doi.org/10.1083/jcb.201608123

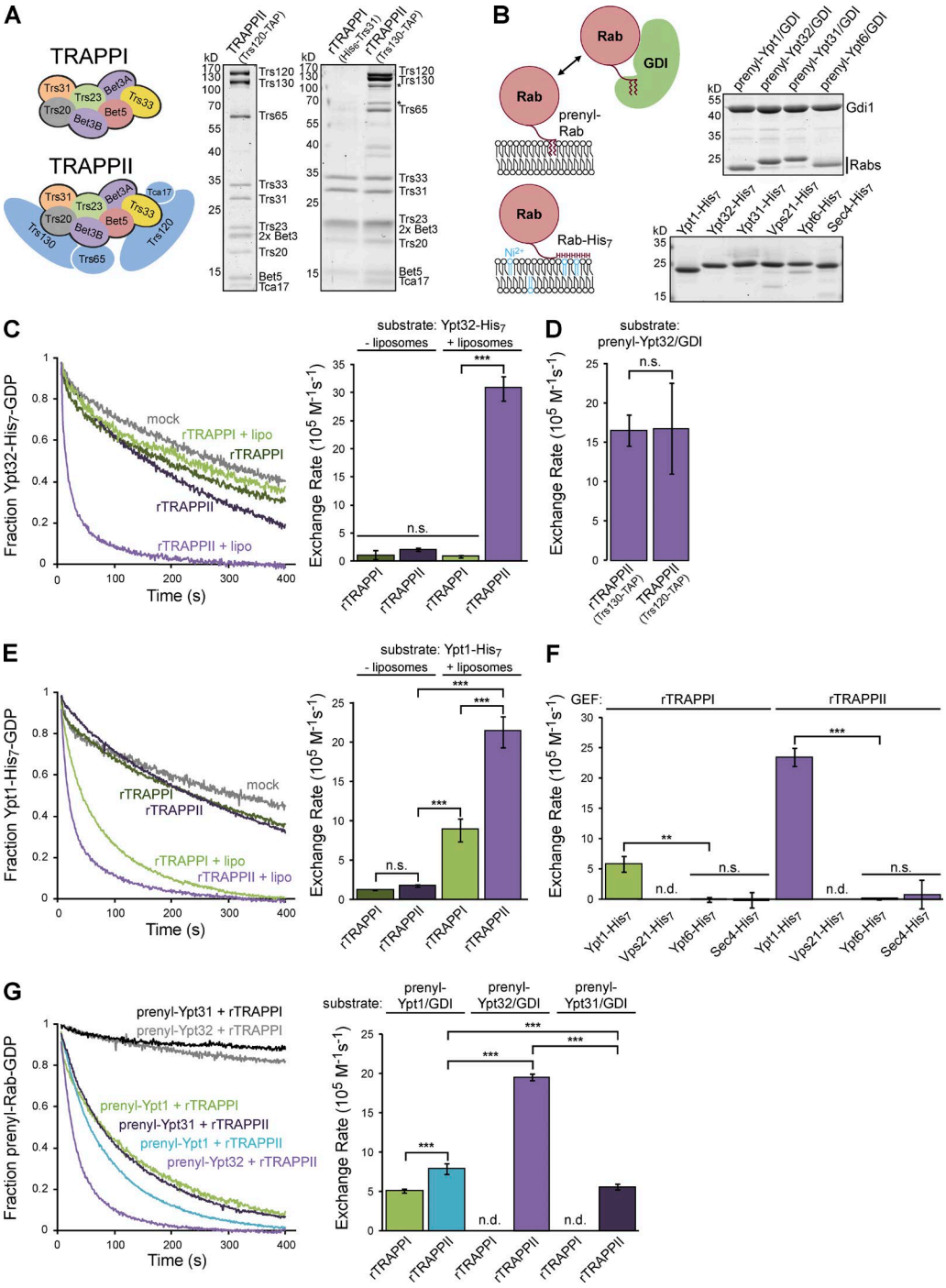

Figure 1. **The TRAPPII complex activates the Rab GTPases Ypt31/32 in a membrane-dependent manner.** (A, left) Subunit composition of TRAPPI and II complexes predicted from structural, biochemical, and yeast two-hybrid data. (right) Endogenous and rTRAPP complexes were purified from yeast or *E. coli*, respectively, using the indicated affinity tag. Asterisk indicates degradation product. (B, left) Schematic of membrane anchoring for prenylated (prenyl) versus His-tagged Rabs. (right) 0.5 µg of each prenylated-Rab/GDI complex and His-tagged Rab substrate used in this study assessed by SDS-PAGE. (C, left) Normalized representative traces showing activation of 250 µM His-tagged Ypt32 by 10 nM rTRAPPI or -II in the presence or absence of synthetic TGN liposomes. "mock" is the buffer-only control for intrinsic exchange of His-tagged Rabs. (right) Rates of rTRAPP-mediated Ypt32-His_7 activation determined from the traces at left. Rates were calculated by subtracting the rate constant for intrinsic exchange (buffer only) from that of TRAPP-mediated exchange. Error bars represent 95% CIs for $n \geq 2$ reactions (without liposomes) or $n \geq 3$ reactions (with liposomes). (D) Rates of prenylated-Ypt32/GDI activation by recombinant versus endogenous TRAPPII in the presence of TGN liposomes. Error bars represent 95% CIs for $n = 3$ reactions. (E, left) Normalized representative traces showing activation of His-tagged Ypt1 by rTRAPPI or -II in the presence or absence of TGN liposomes. (right) Rates of rTRAPP-mediated Ypt1-His_7 activation from the traces at left. Error bars represent 95% CIs for $n \geq 2$ reactions (without liposomes) or $n \geq 4$ reactions (with liposomes). (F) Rates of His-tagged Ypt1, Sec4, and Ypt6 activation by rTRAPPI and -II in the presence of TGN liposomes. Error bars represent 95% CIs for $n \geq 3$ reactions. (G, left) Normalized representative traces showing activation of prenylated-Rab/GDI substrates by 13 nM rTRAPPI or -II in the presence of TGN liposomes. (right) Rates of rTRAPP-mediated prenylated-Rab/GDI activation from the traces at left. Error bars represent 95% CIs for $n \geq 3$ reactions. n.d., not detectable (the Rab was not activated by the GEF, and exponential functions could not be fit to experimental curves). n.s., not significant; **, $P < 0.01$; ***, $P < 0.001$.

2011; Pinar et al., 2015). However, biochemical evidence that TRAPPII directly activates Ypt31/32 is controversial. Although previous studies have reported that TRAPPII catalyzes nucleotide exchange for Ypt31/32 but not Ypt1 (Morozova et al., 2006; Zou et al., 2012), opposing studies have argued that TRAPP complexes are specific GEFs for Ypt1 (Wang et al., 2000; Wang and Ferro-Novick, 2002; Yip et al., 2010), and a recent study found that TRAPPII weakly activates both Ypt1 and Ypt31/32 (Pinar et al., 2015). In all of these studies, the observed TRAPPII GEF activity toward Ypt31/32 appeared low, likely because soluble Rab substrates were used, whereas in cells Rab GTPase activation occurs at the membrane surface of target organelles.

To address this controversy and gain insights into the coordination of trafficking pathways at the TGN, we developed a physiological biochemical reconstitution assay to measure Rab activation. Three innovations distinguish our approach from previous investigations of TRAPPII activity: (1) we used synthetic liposome membranes to provide proper biological context; (2) we purified recombinant TRAPPII (rTRAPPII) from bacteria to avoid copurification of endogenous contaminants; and (3) we used enzymatic synthesis to generate native prenylated-Rab/GDP dissociation inhibitor (GDI) complex substrates. Using this reconstituted system, we demonstrate that the TRAPPII complex is a potent activator of Ypt31/32 requiring both the TRAPPII-specific subunits and the presence of membranes. In contrast to a recently proposed model (Pinar et al., 2015), TRAPPII activates Ypt31/32 via the same active site residues used by TRAPPI to activate Ypt1, representing a remarkable case of active site plasticity. Finally, we show that TRAPPII is recruited to the Golgi through the cooperative action of anionic lipids and the activated form of the Arf1 GTPase. Our findings lead to a model for vesicle biogenesis involving the collaborative action of four essential trafficking regulators: TRAPPII and Ypt31/32 function in a bidirectional feedback loop with Sec7 and Arf1 to orchestrate vesicle formation and prime these vesicles for subsequent transport and tethering.

Results

Reconstitution of physiological RabGEF reactions reveals the Ypt31/32 GEF activity of TRAPPII

TRAPPII is an 11-subunit, 1 MD complex. We used two approaches to prepare stoichiometric TRAPPII complexes. We followed a tandem affinity purification (TAP) procedure used previously to purify endogenous TRAPPII from yeast (Yip et al., 2010; Fig. 1 A). We also produced rTRAPPII purified from *Escherichia coli* (Fig. 1 A), allowing us to test for the possibility of contamination by yeast proteins, which has been a major argument against TRAPPII-catalyzed Ypt31/32 activation (Sacher et al., 2008).

To reconstitute membrane-proximal GEF reactions, we prepared liposome membranes with a composition approximating that of the TGN (Klemm et al., 2009; Richardson et al., 2012). We also prepared two different types of Rab substrates. We developed an enzymatic synthesis procedure to generate recombinant prenylated-Rab/GDI complexes recapitulating the native state of inactive Rab proteins in cells (Fig. 1 B and Fig. S1, A–C), and we engineered Rab substrates in which the two C-terminal prenylated cysteine residues were replaced by a poly-histidine tag to anchor the substrate to liposomes containing nickel ion-binding lipids (Fig. 1 B and Fig. S1 D). As a result of the hydrophobicity of the geranylgeranyl groups, the prenylated-Rab/GDI complexes can only be activated on a membrane surface. In contrast, the Rab-His_7 substrates can be activated either on the membrane surface or in solution if membranes are not included in the reaction, enabling dissection of the contribution of membranes to the GEF reactions. For both types of substrates, the Rab active sites were loaded with a fluorescent GDP analogue (mantGDP) to allow real-time measurements of nucleotide exchange kinetics.

We used these reagents to test the ability of TRAPPII to activate the Ypt32-His_7 substrate. We observed only trace Ypt32 GEF activity in the absence of membranes, consistent with the findings of several previous studies (Fig. 1 C). Remarkably, very robust GEF activity of $\sim 3 \times 10^6$ M^{-1} s^{-1} was observed in the presence of liposomes (Fig. 1 C). Similar behavior was observed with the 81% identical Ypt31-His_7 (Fig. S1 E). Equivalent GEF activity was observed for TRAPPII purified from either yeast or bacterial cells (Fig. 1 D), ruling out the possibility of GEF activity from a copurifying contaminant. The precise location of the TAP-tag in purified TRAPPII complexes was also not important (Fig. 1 D).

We considered that the presence of membranes might enable the smaller TRAPPI complex, representing the core subunits of TRAPPII, to also activate the Ypt32-His_7 substrate. However, TRAPPI was unable to activate Ypt32-His_7 or Ypt31-His_7, even in the presence of membranes (Fig. 1 C and Fig. S1 E). Therefore, the TRAPPII-specific subunits are required for activation of Ypt31/32.

Little consensus exists regarding whether TRAPPII can activate the more distantly related Rab GTPase Ypt1 (44% identical to Ypt32; Morozova et al., 2006; Zou et al., 2012). Both TRAPPI and TRAPPII exhibited robust GEF activity toward Ypt1-His_7 under our assay conditions (Fig. 1 E). Neither TRAPPI nor TRAPPII activated the Rab proteins Vps21 (Rab5 homologue), Sec4 (Rab8 homologue), or Ypt6 (Rab6 homologue; Fig. 1 F and Fig. S1 F), indicating that TRAPPII is a specific GEF for Ypt31/32 and Ypt1.

Membranes stimulated the GEF-catalyzed exchange rates of both Ypt31/32 and Ypt1. At higher concentrations of TRAPPII (>30 nM), membranes were less important for Ypt1 activation, but remained critical for Ypt31/32 activation (unpublished data). The greater membrane dependence of Ypt31/32 activation may explain why previous studies using soluble substrates did not observe TRAPPII-catalyzed Ypt31/32 nucleotide exchange despite successfully producing Ypt1 exchange.

We next asked whether similar GEF activities would be seen on the physiological prenylated-Rab/GDI complex substrates. Remarkably, strong GEF activity was still exhibited by TRAPPII toward Ypt31/32 and Ypt1 (up to 2×10^6 M^{-1} s^{-1}; Fig. 1 G), despite the fact that prenylated Rab substrates must first dissociate from the GDI before nucleotide exchange (Goody et al., 2005). Using these substrates, we observed no intrinsic exchange and no exchange in the absence of membranes (Fig. S1 G), consistent with membrane insertion being a prerequisite for GEF-catalyzed nucleotide exchange. In the presence of excess Gdi1, which drives the equilibrium toward the GDI-bound state, we observed a significant decrease in Rab activation (Fig. S1 H). Addition of excess Mrs6, a Rab escort protein (REP), which should not extract Rabs from membranes, did not significantly decrease activation (Fig. S1 H). These results confirm and extend our observations with the Rab-His_7 substrates and support

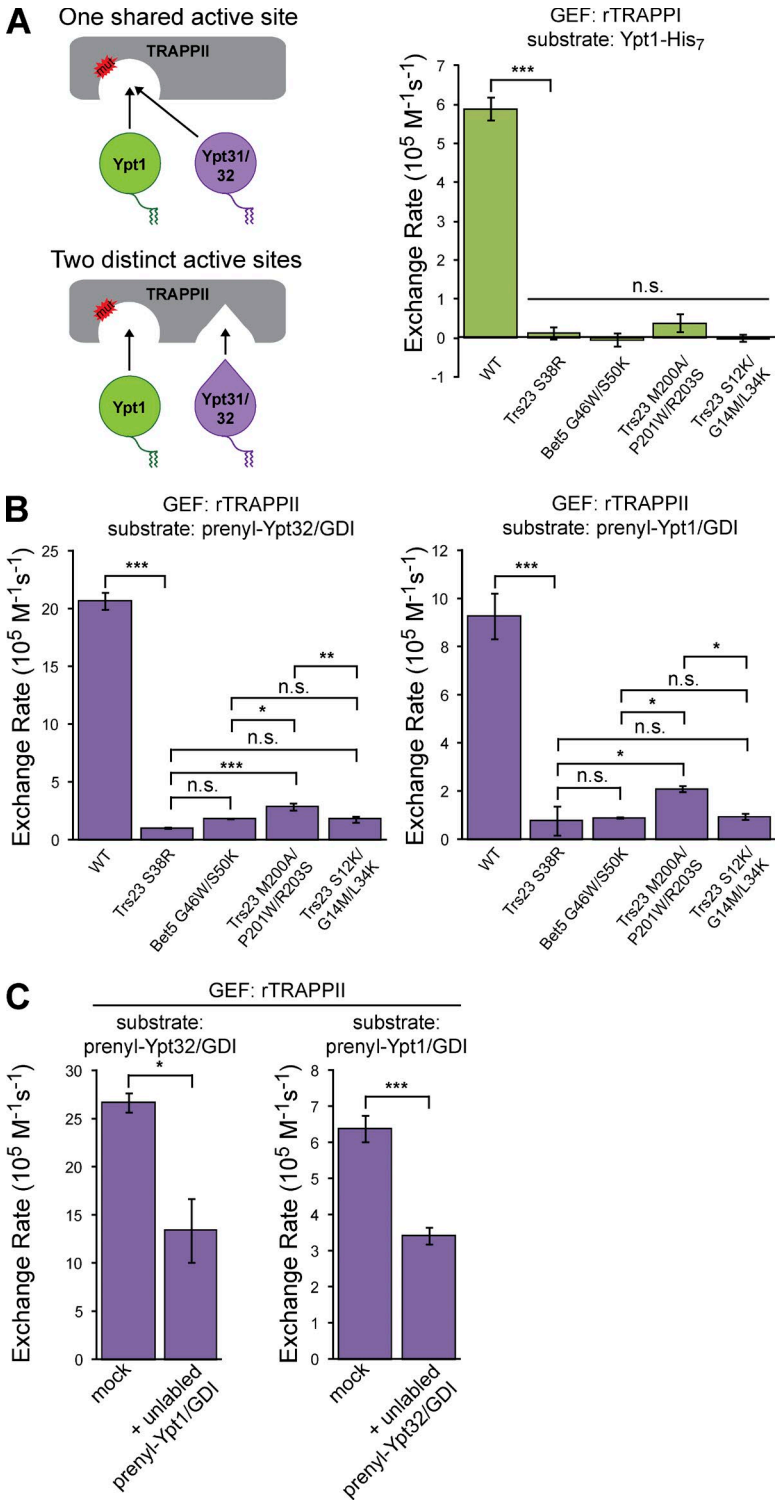

Figure 2. **Ypt31/32 and Ypt1 share an active site in TRAPPII.** (A, left) Schematic depicting two possible mechanisms for TRAPPII-mediated Ypt31/32 activation. (right) The indicated rTRAPPI active site mutants were tested for their ability to activate Ypt1-His_7 in the presence of TGN liposomes. Error bars represent 95% CIs for $n \geq 3$ reactions. (B) rTRAPPII active site mutants were tested for their ability to activate prenylated-Ypt32/GDI and prenylated-Ypt1/GDI in the presence of TGN liposomes. Error bars represent 95% CIs for $n \geq 2$ reactions. (C) rTRAPPII-mediated activation of mantGDP-labeled prenylated-Rab/GDI substrates on TGN liposomes in the absence (mock) or presence of equimolar concentrations of competing unlabeled prenylated-Rab/GDI complexes. Error bars represent 95% CIs for $n \geq 3$ reactions. n.s., not significant; *, $P < 0.05$; **, $P < 0.01$; ***, $P < 0.001$.

the idea that inactive (GDP-bound) prenylated Rabs are in a dynamic equilibrium between membrane- and GDI-bound states.

TRAPPII-specific subunits enable the Ypt1 active site to activate Ypt31/32

The fact that TRAPPII-specific subunits are required for activation of Ypt31/32, but not for activation of Ypt1, raises two mechanistic possibilities (Fig. 2 A). Either the TRAPPII-specific subunits provide an additional active site for Ypt31/32, or they adapt the existing TRAPPI active site to accommodate Ypt31/32 as an additional substrate. Both models have been proposed (Jones et al., 2000; Morozova et al., 2006; Pinar et al., 2015), but neither has been conclusively demonstrated.

To distinguish between these two possibilities, we introduced point mutations known to disrupt activation of Ypt1 in the TRAPPI active site (Fig. 2 A; Cai et al., 2008). If the same active site is used by TRAPPII to activate both Ypt1 and Ypt31/32, these mutations should disrupt activation of each. If a distinct active site is used to activate Ypt31/32, these mutations may not significantly affect Ypt31/32 activation.

Several different TRAPPI active-site point mutations abolished or significantly reduced TRAPPII-catalyzed nucleotide exchange for prenylated Ypt1 and Ypt31/32 (Fig. 2 B and Fig. S2 A). Importantly, none of these mutations affected assembly or composition of TRAPPI or -II complexes (Fig. S2 B). Although it is a formal possibility that mutations in the TRAPPI active site might produce an allosteric effect on a hypothetical secondary active site, our observation that several different TRAPPI active-site mutations exert corresponding effects on Ypt1 and Ypt31/32 activation argues strongly against this possibility. Therefore, the simplest interpretation of these data are that the Ypt1 and Ypt31/32 Rabs are activated by the same active site in the TRAPPII complex.

Certain GEFs are known to activate distinct GTPases using multiple active sites (Feng et al., 2004), but we are unaware of any other instances of a single active site capable of activating multiple distinct GTPases with such a robust exchange rate (10^6 M^{-1} s^{-1}). We therefore tested whether TRAPPII possesses any measurable substrate preference: does TRAPPII preferentially activate Ypt1 or Ypt31/32? In reciprocal competition experiments, the addition of equimolar concentrations of competing unlabeled Rab decreased TRAPPII activation of the mant-labeled Rab by approximately half (Fig. 2 C and Fig. S2 C), indicating that TRAPPII does not display a marked preference for either substrate in vitro. We therefore conclude that Ypt31/32 and Ypt1 are activated by a common catalytic site within the TRAPP core and that the TRAPPII-specific subunits enhance activity toward Ypt1 and expand substrate specificity to enable recognition of Ypt31/32.

The essential function of TRAPPII is to activate Ypt31/32

As our in vitro experiments indicated that TRAPPII is a GEF for both Ypt31/32 and Ypt1, we sought to determine the relative importance of these two TRAPPII activities in cells. We used the extent of Golgi compartment localization as a measurement of Rab activation in vivo. Consistent with previous studies, in wild-type (WT) cells, GFP-Ypt31/32 localized to Sec7-labeled late Golgi/TGN compartments as well as to secretory vesicles at the bud neck and tip (Fig. 3 A). In *trs130Δ33* temperature-sensitive cells at both the permissive (Fig. 3 A) and restrictive temperatures (unpublished data), Ypt31/32 was nearly completely cytosolic. In control experiments, Ypt6, which was not an in vitro substrate for TRAPPII, remained localized to membranes in the *trs130Δ33* mutant at the restrictive temperature (Fig. S3 A). These data indicate that TRAPPII is specifically required for Ypt31/32 activation in cells.

In agreement with a previous study (Morozova et al., 2006), GFP-Ypt1 remained punctate in *trs130Δ33* cells (Fig. 3 B and Fig. S3 B), suggesting that TRAPPII might not be required to activate Ypt1 in cells. However, Ypt1 colocalized significantly less with the late Golgi marker Sec7 in the *trs130Δ33* mutant at the restrictive temperature (Fig. 3, B and C), indicating that TRAPPII contributes to Ypt1 activation at the TGN. Ypt1 activation at earlier Golgi compartments appears to occur independently of TRAPPII function (perhaps via TRAPPI).

Previous studies demonstrated that cell viability in TRAPPII mutants can be rescued by overexpression of WT or constitutively active Ypt31 (Zhang et al., 2002; Sciorra et al., 2005). We replicated this result and further found that the *trs130Δ33* mutant could not be rescued by overexpression of WT or constitutively active Ypt1 (Fig. 3 D). We also tested whether increased expression of Ypt31 or Ypt1 could rescue trafficking defects caused by the *trs130Δ33* mutation. In agreement with a previous study (Zou et al., 2012), overexpression of GTP-locked Ypt31, but not Ypt1, restored trafficking of the SNARE Snc1 in *trs130Δ33* mutant cells (Fig. S3 C). We therefore conclude that, whereas TRAPPII activates both Ypt31/32 and Ypt1 at the late Golgi/TGN, the essential function of TRAPPII in cells is to activate Ypt31/32.

Sec7 activity is required for TRAPPII localization

We sought to identify signals that recruit TRAPPII to the late Golgi/TGN to activate Ypt31/32. A previous study implicated the Arf-GEF Gea2 as a potential recruiter of TRAPPII, but TRAPPII remained properly localized in *gea2Δ* mutant cells (Chen et al., 2011). As Ypt31/32 accumulates at Golgi compartments just downstream of the Arf-GEF Sec7 (McDonold and Fromme, 2014), we asked whether TRAPPII localization is dependent on Sec7 activity. In untreated cells, endogenously tagged TRAPPII (Trs130-mNeonGreen) colocalized well with endogenously tagged Sec7 at late Golgi compartments (Fig. 4 A). In contrast, TRAPPII was significantly mislocalized from Golgi compartments in cells treated with the Golgi Arf-GEF inhibitor brefeldin A (BFA), which inhibits both Gea2 and Sec7 (Fig. 4 A). To separate the effects of Sec7 and Gea2 inhibition, we also tested the compound 6-methyl-5-nitro-2-(trifluoromethyl)-4H-chromen-4-one (MNTC), identified as a likely Sec7 inhibitor in a large-scale screen (Lee et al., 2014). MNTC inhibited Arf activation in vivo (Fig. S3 D) and did not affect the activity of TRAPPII in vitro (Fig. S3 E). Similar to BFA, a brief treatment with MNTC significantly mislocalized TRAPPII from Golgi compartments (Fig. 4 B). To control for the possibility of off-target effects from the inhibitors, we also visualized TRAPPII in *sec7-1* mutant cells. At the restrictive temperature, TRAPPII was significantly more cytoplasmic in the *sec7-1* mutant (Fig. 4 C).

Sec7 remained at Golgi compartments after treatment with either BFA or MNTC (Fig. 4, A, B, and D), suggesting that TRAPPII recruitment depends on the catalytic activity of Sec7 rather than a direct physical interaction. As a small portion of TRAPPII remained at Golgi compartments after each method of Sec7 inhibition, we conclude that Sec7 activity is an important, but not the only, signal mediating TRAPPII localization.

We tested whether Sec7 inhibition correspondingly reduces Ypt31/32 activation. Using Golgi localization as a measurement of Rab activation, we found that Ypt31/32 was significantly mislocalized after treatment with either BFA or MNTC (Fig. 4 D and Fig. S3 F). A decreased population of Ypt31/32 remained at the Golgi after Sec7 inhibition, consistent with our observation that loss of Sec7 activity does not completely abolish TRAPPII recruitment.

Activated Arf1 and anionic lipids cooperate to recruit TRAPPII to the TGN

We next asked whether activated Arf1, the product of Sec7 activity, mediates TRAPPII recruitment. In agreement with a previous study (Chen et al., 2011), TRAPPII was significantly more cytosolic in *arf1Δ* cells (Fig. 5 A and Fig. S4 A). These in vivo results could be explained through indirect effects. Therefore, we used in vitro liposome flotation assays to test whether Arf1 directly interacts with TRAPPII. We observed that TRAPPII is recruited to TGN-like membranes by Arf1-GTP (Fig. 5 B and Fig. S4 B). Therefore, TRAPPII has a direct physical interaction with activated Arf1.

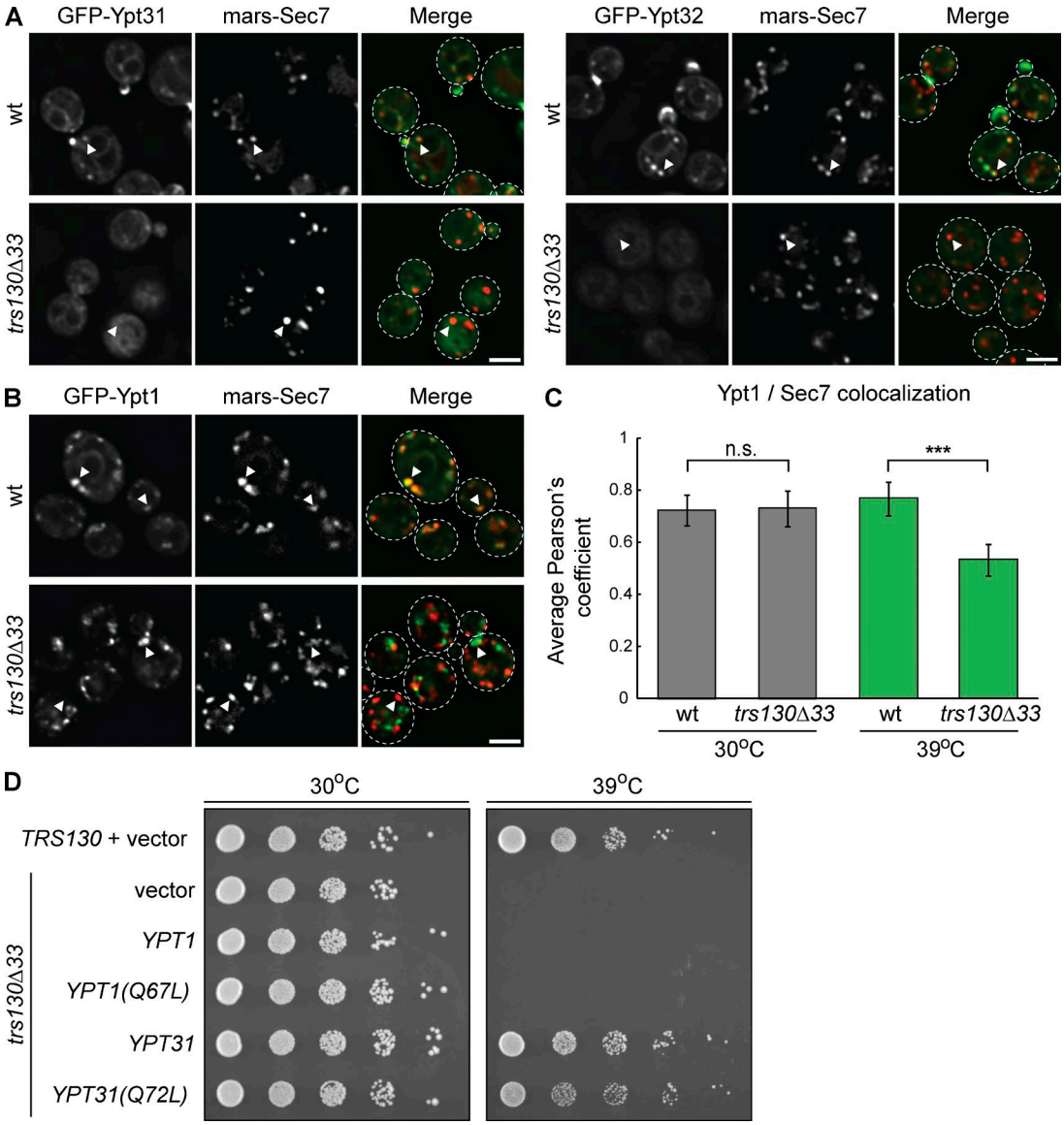

Figure 3. **The essential in vivo function of TRAPPII is to activate Ypt31/32.** (A) Localization of an extra copy of GFP-Ypt31 or GFP-Ypt32 relative to plasmid-borne mRFPmars-Sec7 in WT versus *trs130Δ33* yeast grown at the permissive temperature (30°C). (B) Localization of plasmid-borne GFP-Ypt1 relative to mRFPmars-Sec7 in WT versus *trs130Δ33* yeast after shifting to the restrictive temperature (39°C) for 60 min. (C) Quantification of GFP-Ypt1 and mRFPmars-Sec7 colocalization in WT versus *trs130Δ33* yeast at the permissive temperature or after shifting to the restrictive temperature for 60 min. Error bars represent 95% CIs for $n \geq 25$ cells. (D) Constitutively active or WT Ypt1 and Ypt31 were overexpressed on high copy plasmids to test their ability to rescue growth in temperature-sensitive *trs130Δ33* yeast. Ypt1(Q67L) and Ypt31(Q72L) are GTP-locked mutants. Bars, 2 µm. White arrowheads denote colocalization, or not, of GFP-Rabs and mRFPmars-Sec7 at Golgi compartments. n.s., not significant; ***, $P < 0.001$.

We observed that Arf1 was unable to recruit TRAPPI to membranes (Fig. S4 C), suggesting that the TRAPPII–Arf1 physical interaction is mediated by TRAPPII-specific subunits. We cannot rule out the alternative and unlikely possibility that Arf1-GTP interacts with the TRAPPI core, and the TRAPPII subunits provide additional affinity for the membrane. As Arf1 is present at both early and late Golgi compartments, we hypothesized that additional signals must exist to recruit TRAPPII specifically to the late Golgi/TGN. A previous study suggested that the then-unidentified Ypt31/32 GEF would be a Ypt1 effector (Wang and Ferro-Novick, 2002). We therefore tested whether activated Ypt1 directly stimulates TRAPPII activity, but found that Ypt1 does not promote TRAPPII membrane-binding or GEF activity (Fig. S4, D and E). We also tested the possibility that activated Ypt31/32 functions in a positive-feedback loop by recruiting TRAPPII to membranes, but observed no evidence for such a regulatory circuit (Fig. S4 F).

As late Golgi membranes are comparatively enriched in sterols and anionic phospholipids (Klemm et al., 2009; Bigay and Antonny, 2012), we tested whether the lipid composition of TGN membranes cooperates with active Arf1 to localize TRAPPII. Arf1 did not recruit TRAPPII to membranes containing only neutral TGN lipids (Fig. 5 B). In contrast, Arf1 robustly recruited TRAPPII to anionic TGN membranes containing phosphatidylserine (PS), phosphatidic acid, phosphatidylinositol (PI), and PI 4-phosphate (PI(4)P). At concentrations representative of TGN membranes, no single anionic lipid was sufficient for TRAPPII recruitment (unpublished data). We conclude that the overall pool of anionic lipids in the synthetic TGN membranes, rather than

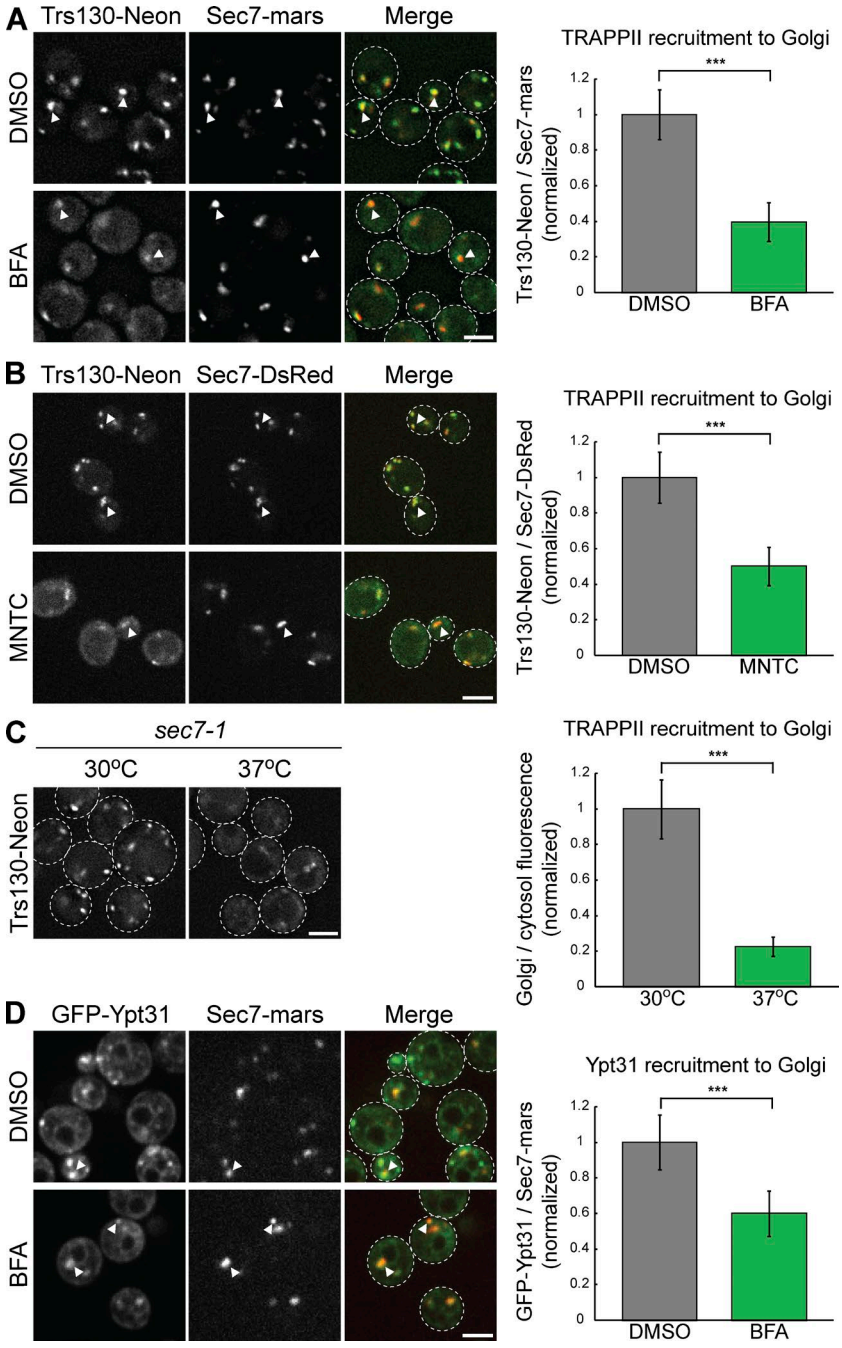

Figure 4. **Sec7 activity is required for TRAPPII recruitment and Ypt31/32 activation at the late Golgi/TGN.** (A, left) Localization of Trs130-mNeonGreen relative to the late Golgi marker Sec7-mRFPmars in cells treated with DMSO (vehicle control) or BFA for 15 min. (right) Recruitment of TRAPPII to Golgi compartments was measured by quantifying the ratio of Trs130-mNeonGreen fluorescence to that of Sec7-mRFPmars in Sec7-mRFPmars puncta. Error bars represent 95% CIs for $n = 55$ (DMSO) or $n = 21$ (BFA-treated) compartments. (B, left) Localization of Trs130-mNeonGreen relative to Sec7-6xDsRed in cells treated with DMSO (vehicle control) or MNTC for 10 min. (right) Recruitment of TRAPPII to Golgi compartments was measured as in A. Error bars represent 95% CIs for $n = 55$ (DMSO) or $n = 42$ (MNTC-treated) compartments. (C, left) Localization of Trs130-mNeonGreen in a *sec7-1* mutant after shifting to the restrictive temperature for 20 min. (right) Line trace quantification of cytosolic and Golgi localization of TRAPPII. Error bars represent 95% CIs for $n = 7$ (30°C) or $n = 9$ (37°C) cells. (D, left) Localization of GFP-Ypt31 relative to Sec7-mRFPmars in cells treated with DMSO or BFA for 15 min. (right) Recruitment of Ypt31 to Golgi compartments was measured as in A and B. Error bars represent 95% CIs for $n = 58$ (DMSO) or $n = 37$ (BFA-treated) compartments. Bars, 2 µm. White arrowheads denote colocalization of TRAPPII or Ypt31 with Sec7 at Golgi compartments. ***, $P < 0.001$.

a single specific lipid, promotes TRAPPII localization. This is consistent with a previous study proposing that TRAPP complexes are directed to Golgi membranes by electrostatic interactions between anionic lipids and a positively charged surface on the core subunit Bet3 (Kim et al., 2005).

We next tested whether Arf1 and anionic lipids cooperate to stimulate TRAPPII activation of Ypt31/32 at the membrane surface. Active Arf1 dramatically enhanced TRAPPII-catalyzed Ypt31/32 nucleotide exchange in an anionic lipid-dependent manner (Fig. 5 C and Fig. S4 G). This result indicates that membrane recruitment of TRAPPII correlates strongly with TRAPPII GEF activity.

We examined whether anionic lipids contribute to TRAPPII recruitment in cells. Given the genetic links among TRAPPII, Ypt31/32, and the PI(4)P kinase Pik1, as well as established roles for PI(4)P in secretory vesicle formation and trafficking (Sciorra et al., 2005; D'Angelo et al., 2008; Daboussi et al., 2012), we tested whether Pik1 function is important for TRAPPII recruitment. TRAPPII localization was not significantly altered in *pik1-139* ts cells (Fig. S4 H). As PI(4)P comprises only ∼1% of total TGN lipids, this result is consistent with the hypothesis that TRAPPII is recruited to the membrane by general anionic lipids at the late Golgi/TGN and that PI(4)P specifically does not play an important role in recruiting TRAPPII. The late Golgi/TGN-localized flippase Drs2 regulates protein sorting by exposing anionic PS in the cytosolic leaflet (Hankins et al., 2015); and the *drs2Δ* mutation is synthetically lethal with *ypt31Δ*, *arf1Δ*, and TRAPPII mutations (Fig. S4 I; Chen and Graham, 1998; Sciorra et al., 2005). TRAPPII was partially mislocalized in

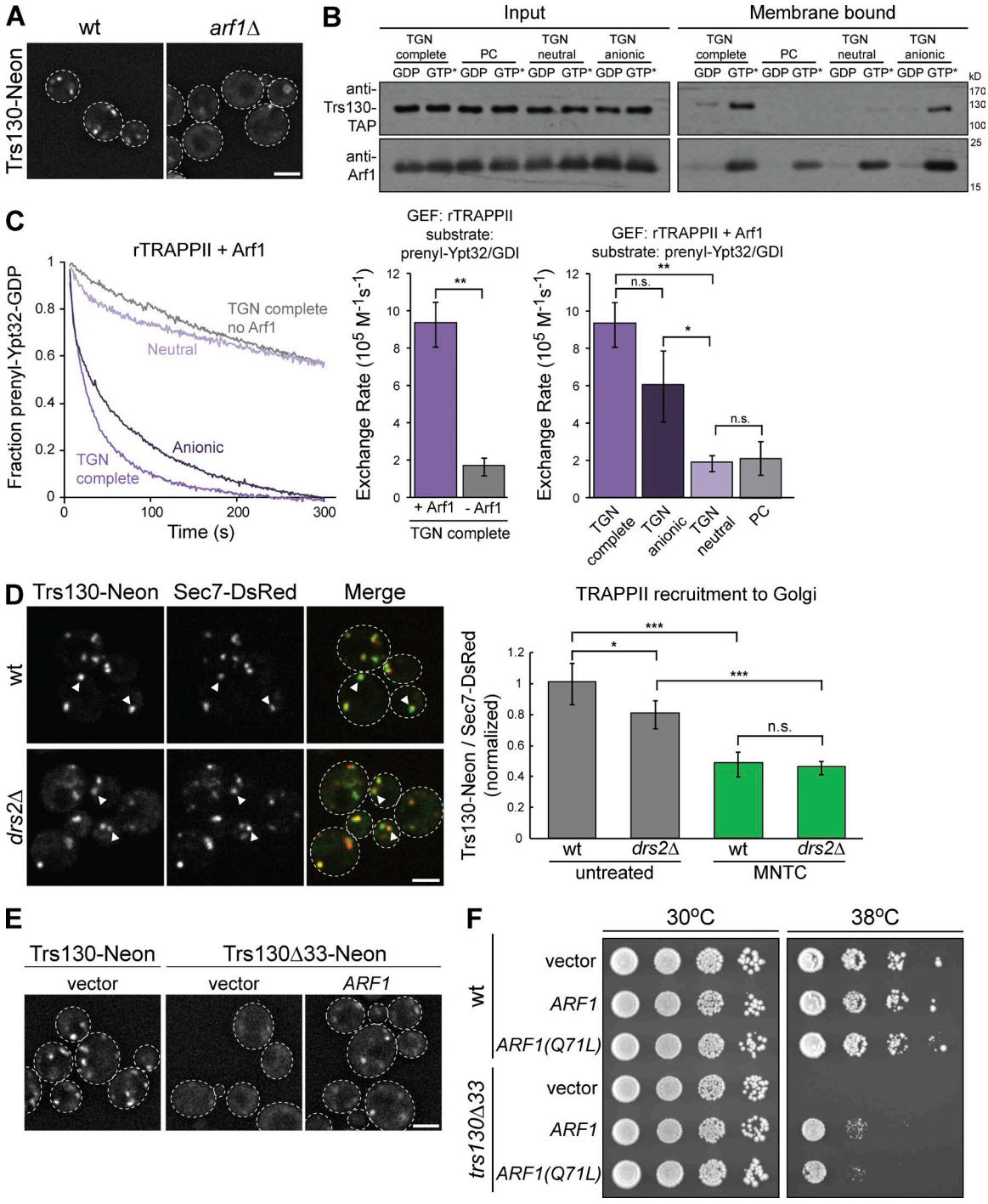

Figure 5. **Activated Arf1 and anionic lipids cooperate to recruit TRAPPII to membranes in vitro and in vivo.** (A) Localization of Trs130-mNeonGreen in WT versus *arf1Δ* yeast grown at 30°C. (B) Liposome flotation assay testing TRAPPII recruitment to different membranes by activated myristoylated-Arf1. Proteins were visualized by Western blot. Liposomes do not contain Ni^{2+}-DOGS (see Materials and methods). GTP* indicates GMP-PNP. (C, left) Representative normalized traces showing rTRAPPII-catalyzed prenylated-Ypt32/GDI activation in the presence or absence of activated myristoylated-Arf1 on synthetic TGN liposomes, liposomes containing only anionic or neutral TGN lipids, or PC liposomes. Liposomes do not contain Ni^{2+}-DOGS. (right) Rates of Ypt32 activation determined from the traces at left. Error bars represent 95% CIs for $n \geq 3$ reactions. (D, left) Localization of Trs130-mNeonGreen relative to the late Golgi marker Sec7-6xDsRed in WT versus *drs2Δ* yeast grown at 30°C. (right) Recruitment of TRAPPII to Golgi compartments was measured by quantifying the ratio of Trs130-mNeonGreen to Sec7-6xDsRed in Sec7-6xDsRed puncta. Recruitment was measured in untreated cells and cells treated with MNTC for 10 min. Error bars represent 95% CIs for $n \geq 62$ compartments. (E) Arf1 expressed on a low-copy plasmid partially rescues localization of *trs130Δ33* mutant TRAPP complexes in yeast grown at 30°C. (F) Constitutively active or WT Arf1 was expressed on low-copy plasmids to test the ability of Arf1 to rescue growth in temperature-sensitive *trs130Δ33* mutant cells. Arf1(Q71L) is a GTP-locked mutant. Bars, 2 µm. White arrowheads denote colocalization of Trs130-mNeonGreen and Sec7-DsRed at Golgi compartments. n.s., not significant; *, $P < 0.05$; **, $P < 0.01$; ***, $P < 0.001$.

drs2Δ cells (Fig. 5 D), consistent with PS playing a minor role in recruiting TRAPPII to the late Golgi/TGN.

In support of our finding that Arf1 recruits TRAPPII to the TGN, overexpression of Arf1 partially restored the punctate localization of Trs130Δ33 (Fig. 5 E and Fig. S4 J). Furthermore, overexpression of either WT or constitutively active Arf1 partially rescued viability in *trs130Δ33* mutant cells (Fig. 5 F).

Collectively, these results demonstrate that activated Arf1 plays a major role in recruiting TRAPPII to the membrane surface. Given the broad distribution of Arf1 throughout the Golgi, another factor must provide additional specificity for the late Golgi/TGN. Our results suggest that anionic lipids are a likely candidate for such a specificity factor, though additional factors may also play a role.

TRAPPII is recruited to the TGN immediately after Sec7, coinciding with the Ypt1 to Ypt31/32 transition

To further investigate the role of TRAPPII as a key mediator of TGN vesicle formation, we used live-cell imaging to establish the dynamics of TRAPPII relative to other important regulators at the TGN. Because tagged Arf1 is nonfunctional (Jian et al., 2011), we tracked TRAPPII dynamics relative to Sec7. In agreement with Sec7-activated Arf1 acting as a major TRAPPII recruiter, TRAPPII accumulated at the TGN immediately downstream of Sec7 (Fig. 6 A). Furthermore, TRAPPII colocalized well with both Sec7 and the FAPP1 pleckstrin homology (PH) domain, a coincidence detector of Arf1 and PI(4)P (Fig. 6 B and Fig. S5 A). TRAPPII showed more limited overlap with the early Golgi proteins Gea1 and Vrg4, as well as the medial/late Golgi–localized Rab Ypt6, which has been previously implicated as a TRAPPII interactor in metazoans (Gillingham et al., 2014). These data indicate that the TGN is the primary localization site of TRAPPII in yeast cells.

As expected, Ypt31/32 accumulated at the late Golgi directly after TRAPPII recruitment (Fig. 6, C–E; and Fig. S5 B). In contrast, Ypt1 was present at the Golgi before TRAPPII appeared, and Ypt1 levels at the Golgi began to decline as TRAPPII arrived (Fig. 6, C–E). Ypt1 and Ypt31/32 function in a RabGAP cascade, with activated Ypt32 recruiting the RabGAP Gyp1 to inactivate Ypt1 (Rivera-Molina and Novick, 2009), which could explain the inverse relationship between Ypt1 and TRAPPII accumulation. We therefore examined the dynamics of TRAPPII and Ypt1 in *gyp1Δ* mutant cells and found that loss of Gyp1 significantly increased the overlap of Ypt1 and TRAPPII (Fig. S5 C). Overall, our data indicate that TRAPPII activates a small pool of Ypt1 at the late Golgi, but TRAPPII activation of Ypt31/32 ultimately inactivates Ypt1 via recruitment of Gyp1 (Fig. 6 E).

Discussion

The Rab GTPase Ypt31/32 (Rab11) is a key driver of secretory vesicle formation and subsequent vesicle transport. Despite the significance of Ypt31/32 and other Rab11 homologues in mediating traffic in the secretory and endocytic recycling pathways, there has been no clear consensus regarding the identity of the GEF that activates Ypt31/32.

We now present unambiguous evidence that the TRAPPII complex is a GEF for Ypt31/32. The TRAPPI complex was unable to catalyze Ypt31/32 activation, suggesting that TRAPPII-specific subunits may contact Ypt31/32 to enable nucleotide exchange. Robust activation of Ypt31/32 also required membranes. An interesting possibility is that the TRAPPII complex may be autoinhibited in solution and membrane association mediated by TRAPPII-specific subunits may induce a conformational change enabling Ypt31/32 activation. Indeed, the activities of multiple GEFs are regulated by autoinhibition, albeit by diverse mechanisms (Sondermann et al., 2004; DiNitto et al., 2007; Richardson et al., 2012; Stalder and Antonny, 2013).

We also discovered that TRAPPII is recruited to membranes by activated Arf1 (Fig. 7 A). As active Arf1 is present throughout the Golgi, additional signals must exist to direct TRAPPII specifically to the late Golgi. Consistent with genetic interactions between TRAPPII and the PS lipid flippase Drs2, we found that anionic lipids were important for TRAPPII recruitment and Ypt31/32 activation in vitro. Late Golgi/TGN membranes are significantly enriched in negatively charged phospholipids as compared with the cis-Golgi (van Meer et al., 2008; Bigay and Antonny, 2012). Cargo sorting and vesicle formation at the late Golgi/TGN is strongly influenced by the composition and organization of membrane lipids (De Matteis and Luini, 2008; Papanikou and Glick, 2014), and PS has been shown to be required for proper sorting from the TGN to the plasma membrane (Hankins et al., 2015). Peripheral membrane proteins regulating late secretory and endocytic traffic, such as the ArfGAP Gcs1 or the Ypt7 GEF Mon1-Ccz1, are recruited through electrostatic interactions with anionic phospholipids (Xu et al., 2013; Cabrera et al., 2014). In contrast, other transport machinery, such as the Sec4 GEF Sec2 or the motor protein Myo2, are recruited to membranes through specific interactions with the signaling lipid PI(4)P (Mizuno-Yamasaki et al., 2010; Santiago-Tirado et al., 2011). No single lipid was sufficient for TRAPPII recruitment; moreover, TRAPPII was only partially mislocalized in *drs2Δ* cells. As PS comprises only a fraction of the anionic lipids at the late Golgi (Klemm et al., 2009), we favor a model in which the total pool of negatively charged phospholipids at the TGN mediates TRAPPII membrane-binding specificity, but further studies are needed to establish the precise lipid requirements.

Time-lapse imaging data (Rivera-Molina and Novick, 2009; McDonold and Fromme, 2014; Kim et al., 2016) have established a Rab GTPase transition from Ypt1 to Ypt31/32 at the late Golgi. Moreover, perturbations in Ypt1 or Ypt31 activity alter the dynamics of Golgi maturation (Kim et al., 2016), indicating that these Rab GTPases are essential drivers of cisternal progression. At the late Golgi, cargo sorting occurs as Ypt31/32 levels peak, suggesting that the handoff between Ypt1 and Ypt31/32 is a key signal in vesicle formation and trafficking (McDonold and Fromme, 2014). Although previous studies (Cai et al., 2008; Lynch-Day et al., 2010) and our biochemical data suggest that TRAPPII can directly catalyze exchange for Ypt1, TRAPPII is recruited to Golgi compartments downstream of Ypt1 peak levels and does not play an essential role in Ypt1 activation. Moreover, Ypt1 levels at the Golgi declined concomitant with TRAPPII and Ypt31/32 accumulation because of recruitment of the Ypt1 GAP Gyp1 as a Ypt31/32 effector. Though TRAPPII did not exhibit an obvious preference for Ypt31/32 over Ypt1 in our biochemical assays, it is possible that additional TRAPPII-interacting partners influence substrate specificity to favor Ypt31/32 activation in vivo. Overall, our data indicate that TRAPPII triggers the transition from Ypt1

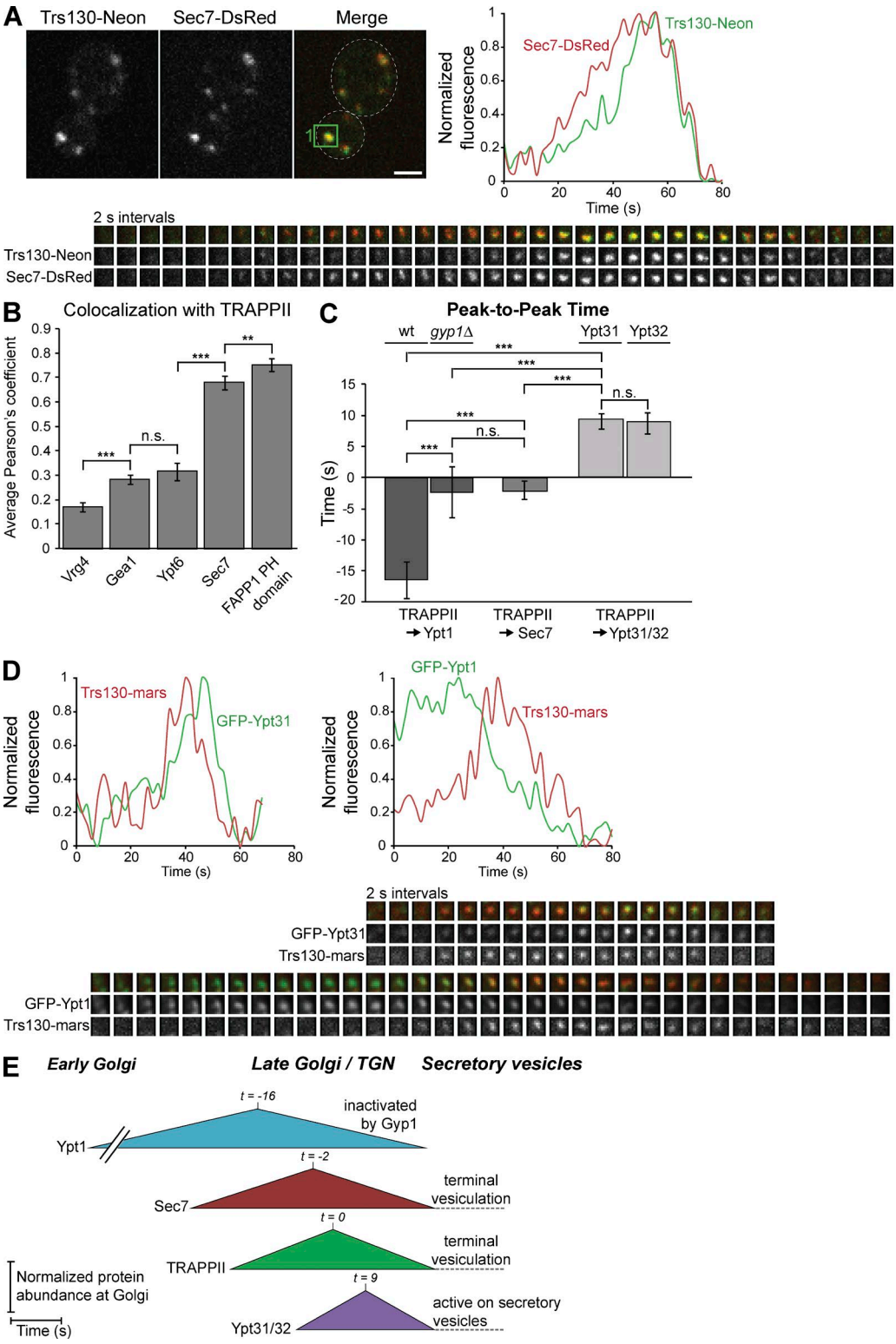

Figure 6. **TRAPPII is recruited to the late Golgi immediately after Sec7, coinciding with the Ypt1 to Ypt31/32 transition.** (A, bottom) Time-lapse imaging series (2-s intervals) of an example single Golgi compartment (the green boxed region in the Merge panel) in live cells harboring endogenous Trs130-mNeonGreen and Sec7-6xDsRed tags. (top right) Normalized quantification of the Trs130-mNeonGreen and Sec7-6xDsRed signals in the boxed region. (B) Colocalization analysis of TRAPPII (Trs130-mNeonGreen or Trs130-3xmRFPmars) with the early Golgi proteins GFP-Vrg4 and Gea1-3xmRFPmars, the medial/late Golgi localized Rab GFP-Ypt6, the late Golgi/TGN marker Sec7-6xDsRed, and GFP-hFAPP1 PH domain, a coincidence detector of PI(4)P and Arf1. Error bars represent 95% CIs of $n \geq 24$ cells. (C) Quantification of peak-to-peak times for each indicated pair of proteins. Error bars represent 95% CIs for $n \geq 10$ series. (D) Time-lapse imaging series (2-s intervals) and normalized quantification of GFP-Ypt31 or GFP-Ypt1 and Trs130-3xmRFPmars for a single Golgi compartment as in A. (E) Model for the dynamics of TRAPPII relative to Ypt1, Sec7, and Ypt31/32 at the late Golgi. $t = 0$ is set to peak TRAPPII recruitment. Regions of interest for time-lapse imaging series are 0.7 × 0.7 µm. Bar, 2 µm. n.s., not significant; **, $P < 0.01$; ***, $P < 0.001$.

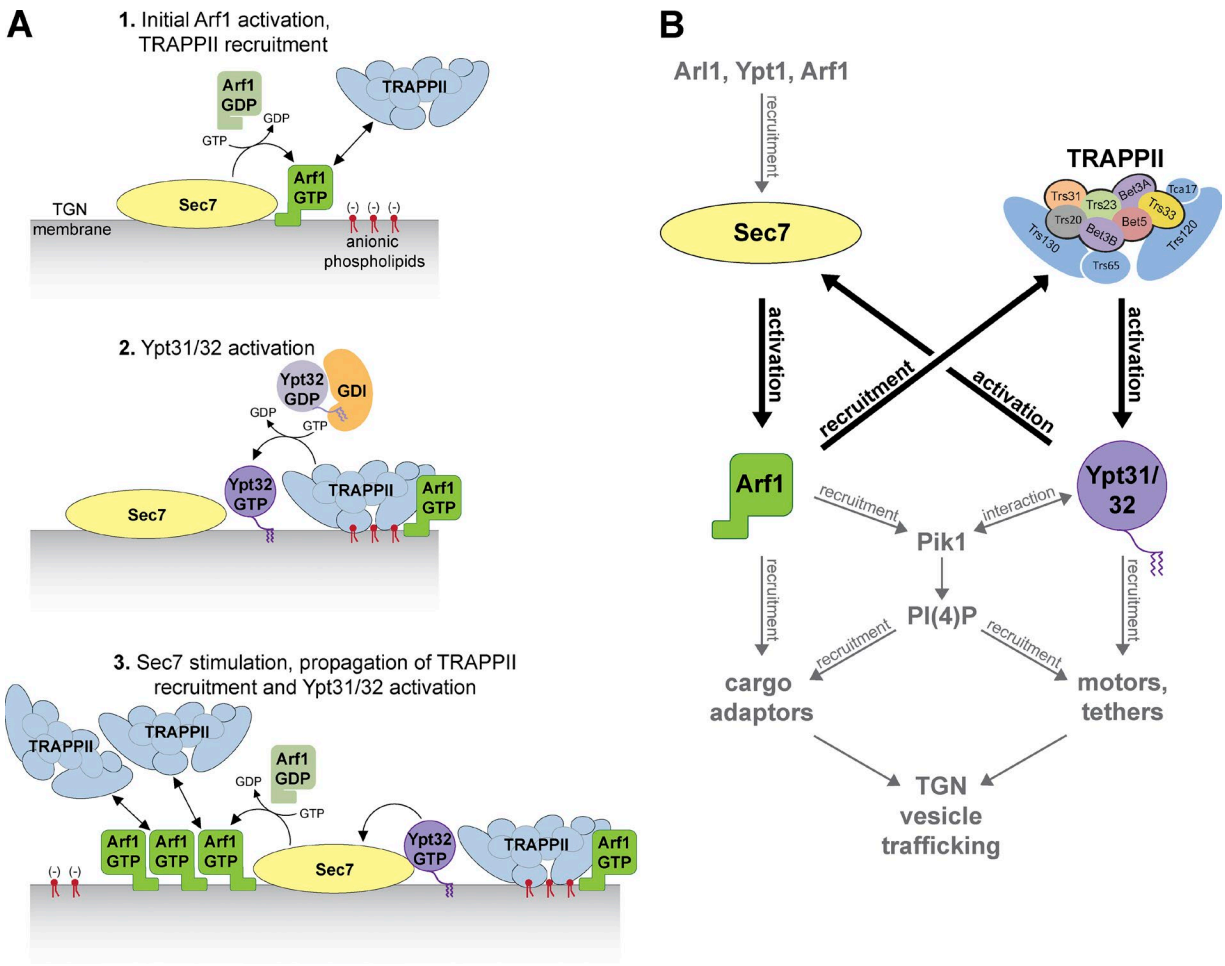

Figure 7. **Bidirectional feedback between TRAPPII-Ypt31/32 and Sec7-Arf1 orchestrates vesicle trafficking at the TGN.** (A) Model for the ordered series of events leading to vesicle formation at the TGN, highlighting the roles of Arf1 in recruiting TRAPPII and Ypt31/32 in stimulating Sec7 activity. (B) Model for the roles of functional physical interactions among TRAPPII, Ypt31/32, Sec7, and Arf1. Interactions of Pik1 homologues with Arf1 and Rab11 have been reported in mammalian and insect cells.

to Ypt31/32, therefore regulating cisternal maturation and initiating vesicle biogenesis at the TGN.

The data reported in this study suggest that TRAPPII makes the molecular decision to activate Ypt31/32 by monitoring the status of other Golgi trafficking regulators. Previous work has shown that Ypt31/32 dramatically enhances Sec7-catalyzed Arf1 nucleotide exchange (McDonold and Fromme, 2014). We propose a bidirectional feedback model in which activated Arf1, a signal of outgoing Golgi traffic, recruits TRAPPII to activate Ypt31/32 on nascent vesicles, which in turn stimulates Sec7-mediated Arf1 activation (Fig. 7 B). GTP-bound Arf1 and Ypt31/32 subsequently recruit downstream effectors, including cargo adaptors, motor proteins, and the GEF Sec2, which activates the Rab Sec4 to promote vesicle tethering at the plasma membrane. The Sec7-TRAPPII bidirectional feedback loop therefore generates vesicles while simultaneously ensuring recruitment of the machinery required for downstream vesicle transport and tethering. Given the conservation of Ypt31/32, TRAPPII, Sec7, and Arf1 in other organisms and that TRAPPII has been shown to function upstream of Ypt31/32 homologues in other organisms (Robinett et al., 2009; Qi et al., 2011; Westlake et al., 2011; Pinar et al., 2015), we expect that a similar mechanism may regulate secretory and endocytic recycling vesicle formation in most eukaryotes.

Materials and methods

Strains and plasmids

All yeast strains and plasmids were constructed using standard techniques and are described Tables S1 and S2.

Antibodies and inhibitors

The anti-Arf1 rabbit polyclonal antibody was a gift from the Schekman laboratory (University of California, Berkeley, Berkeley, CA) and used at a 1:4,000 dilution. The anti-TAP tag rabbit polyclonal antibody used to detect Trs130-TAP was purchased from Thermo Fisher Scientific and used at 1:1,000. The anti-His_6 mouse monoclonal antibody was purchased from Covance and used at 1:1,000.

To test the role of Sec7 activity in TRAPPII recruitment to Golgi compartments in cells, 0.075 mg/ml BFA (Sigma-Aldrich) or 20–40 µM MNTC (MolPort) was added to growth media for 10–15 min before imaging. We determined that the minimum effective concentration of MNTC in cells was <20 µM. In control experiments, cells were treated with equal volumes of DMSO (vehicle).

Protein purification

All *E. coli* purifications used Rosetta2 cells (EMD Millipore). The genes for Rab GTPases and *GDI1* were amplified from SEY6210 yeast

genomic DNA and cloned into the pGEX-6P vector backbone with N-terminal GST-tags. GST-Rab constructs were generated with and without C-terminal His_7 tags. His-tagged Rabs were designed so that the C-terminal cysteine residues were replaced by a His_7 tag to allow membrane anchoring. The expression vectors were transformed into Rosetta2 *E. coli* cells and grown in 1–4 liters of Terrific broth (TB) to an OD of ∼3.0. The temperature was then reduced to 18°C, and protein expression was induced overnight with 300 µM IPTG. Cells were lysed by sonication in lysis buffer (1× PBS, 2 mM $MgCl_2$, 5 mM β-mercaptoethanol [BME], and 1 mM PMSF), and the lysate was cleared by centrifugation. GST-tagged proteins were affinity purified using glutathione resin (G-Biosciences) followed by overnight treatment at 4°C with PreScission (3C) protease in PreScission buffer (50 mM Tris-HCl, pH 7.5, 150 mM NaCl, 1 mM EDTA, 2 mM $MgCl_2$, and 1 mM DTT) to remove the GST tag. Cleavage of the GST tag eluted the proteins from the resin, and the purified proteins were snap frozen in liquid N_2 and stored at −80°C.

Purified Rabs were labeled with mantGDP (BIOLOG Life Science Institute) as previously described (Itzen et al., 2007) to measure nucleotide exchange in GEF activity assays. 1 mg Rab was mixed with fivefold molar excess mantGDP in PreScission buffer with twofold molar excess EDTA over $MgCl_2$ for 2 h at room temperature. The exchange reaction was stopped with the addition of excess $MgCl_2$. MantGDP-loaded Rabs with C-terminal His_7 tags were buffer exchanged into HKM buffer (20 mM Hepes, pH 7.4, 150 mM KOAc, 2 mM $MgCl_2$, and 1 mM DTT), concentrated to 1.0 mg/ml, and frozen at −80°C. Full-length mantGDP-labeled Rabs without His_7 tags were buffer exchanged into prenylation buffer and immediately used to generate prenylated-Rab/GDI complexes.

MRS6 was cloned into the pET28 vector backbone with an N-terminal His_6 tag, and *BET2* and *BET4* were cloned into the pCDFDuet-1 backbone with a His_6 tag upstream of *BET2*. After protein expression, cells grown in 1–8 liters TB were lysed in lysis buffer (40 mM Tris-HCl, pH 8.0, 300 mM NaCl, 10% glycerol, 10 mM imidazole, 2 mM $MgCl_2$, 5 mM BME, and 1 mM PMSF), and His-tagged proteins were affinity purified using Ni-NTA resin (QIAGEN). Proteins were eluted using Elution buffer (Lysis buffer with 250 mM imidazole) and further purified with gel-filtration chromatography using a Superdex 200 10/300 GL column (GE Healthcare) equilibrated with Prenylation buffer.

rTRAPPI was expressed from a single pCOLADuet-1 vector containing all six genes (*TRS33*, *TRS31*, *TRS23*, *BET3*, *TRS20*, and *BET5*; pLT14) with a cleavable His_6 tag upstream of *TRS31*. rTRAPPI was purified from 1–2 liters TB in the same manner as His_6-Mrs6 and His_6-Bet2/Bet4, with TEV protease treatment before gel filtration to remove the His_6 tag. For consistency across purified endogenous and rTRAPP complexes, calmodulin elution buffer (25 mM Tris-HCl, pH 8.0, 300 mM NaCl, 5% glycerol, 0.1% CHAPS detergent, 1 mM magnesium acetate, 1 mM imidazole, 20 mM EGTA, and 1 mM DTT) was used for gel filtration.

rTRAPPII was purified by coexpressing from the following three plasmids in Rosetta2 cells: an rTRAPPI plasmid with the His_6 tag removed from *TRS31* (pLT21), pETDuet-1 with *TRS120* and *TCA17* (pLT16), and pCDFDuet-1 with *TRS130-TAP* and *TRS65* (pLT36). The TAP tag used in this study consists of a calmodulin-binding peptide separated from a protein A tag by a TEV protease site. rTRAPPII was purified from cells grown in 8 liters TB lysed in lysis buffer (20 mM Hepes, pH 7.4, 300 mM NaCl, 5% glycerol, 1% CHAPS, 2 mM $MgCl_2$, 1 mM DTT, 50 mM NaF, 0.1 mM Na_3VO_4, 1 mM PMSF, and 1× Protease Inhibitor Cocktail [Roche]). The following steps were performed at 4°C. The lysate was incubated with Sepharose 6B (Sigma-Aldrich) for 30 min to remove any proteins that bind nonspecifically to Sepharose. The cleared lysate was then incubated with IgG Sepharose (GE Healthcare) for 3 h to isolate protein A–tagged rTRAPPII. The IgG Sepharose was washed with IPP300 buffer (25 mM Tris-HCl, pH 8.0, 300 mM NaCl, 5% glycerol, 0.1% CHAPS, and 1 mM DTT) followed by TEV cleavage buffer (IPP300 with 0.5 mM EDTA), and the protein A tag was cleaved by overnight treatment with TEV protease. Eluted protein was diluted in calmodulin binding buffer (25 mM Tris-HCl, pH 8.0, 300 mM NaCl, 5% glycerol, 0.1% CHAPS, 1 mM magnesium acetate, 1 mM imidazole, 2 mM $CaCl_2$, and 1 mM DTT) and incubated with Calmodulin Sepharose (GE Healthcare) for 2 h at 4°C. rTRAPPII was eluted with calmodulin elution buffer and further purified with anion-exchange chromatography using a MonoQ 5/50 GL column (GE Healthcare) equilibrated in calmodulin elution buffer.

Endogenous TRAPPII was purified from 12 liters log-phase yeast expressing Trs120-TAP. Yeast were lysed using a BeadBeater (Biospec Products), and TRAPPII was purified from the lysate using the same protocol as for rTRAPPII without the final anion-exchange chromatography step. As previously reported (Yip et al., 2010), we found that the addition of CHAPS detergent to all purification buffers significantly increased the final yield of TRAPPII. Samples from each TRAPP preparation were run on a 15% SDS-PAGE gel, strained for total protein with BioSafe Coomassie (Bio-Rad Laboratories), and imaged on an Odyssey instrument (LI-COR Biosciences). All images of Coomassie gels were processed with the despeckle filter in ImageJ (National Institutes of Health). Subunit composition was quantified using ImageJ, and each preparation contained nearly stoichiometric levels of all subunits, including two copies of Bet3.

Myristoylated-Arf1 and -Arl1 were purified as previously described (McDonold and Fromme, 2014). In brief, Arf1 or Arl1 were coexpressed with *N*-myristoyl transferase in *E. coli* in the presence of myristate (Sigma-Aldrich). Cells grown in 1 liter Luria-Bertani broth were lysed in lysis buffer (25 mM Tris-HCl, pH 7.5, 100 mM NaCl, 1 mM $MgCl_2$, 10 mM BME, and 1 mM PMSF), and the lysate was incubated with SP-sepharose (GE Healthcare) to clear contaminating proteins. Unbound protein was purified by anion-exchange and gel-filtration chromatography followed by hydrophobic interaction chromatography using a HiTrap Phenyl HP column (GE Healthcare). Sar1 was a gift from the Miller laboratory (Medical Research Council Laboratory of Molecular Biology, Cambridge, England, UK).

Generation of prenylated-Rab/GDI complexes

Purified mantGDP-labeled Rab, Gdi1, His_6-Mrs6, and His_6-Bet2/Bet4 were mixed in a 10:10:1:1 ratio with sixfold molar excess geranylgeranyl pyrophosphate (Cayman Chemical) in prenylation buffer (20 mM Hepes, pH 7.4, 150 mM NaCl, 2 mM $MgCl_2$, 20 µM mantGDP, and 1 mM DTT) and incubated at 37°C for 60 min to allow prenylation. After prenylation, imidazole was added to a final concentration of 10 mM to prevent nonspecific binding to Ni-NTA resin. A 0.1 volume of equilibrated Ni-NTA resin was then added, and the mixture was incubated at 4°C for 60 min to deplete the His_6-Mrs6 and His_6-Bet2/Bet4. The supernatant, containing prenylated-Rab/GDI complexes, was further purified using gel-filtration chromatography. Fractions containing stoichiometric prenylated-Rab/GDI complexes were pooled and used as substrates in GEF activity assays. Prenylated-Rab/GDI complexes were also prepared using nonfluorescent GDP to test Rab-mediated recruitment of TRAPPII in membrane binding and GEF assays. See Fig. S1 for a schematic and example of samples taken during the generation of prenylated-Rab/GDI complexes.

Membrane binding assays were performed to test whether Rabs were prenylated (see Liposome pelleting assays). Rabs also bound membranes in liposome floatation assays (Fig. S4) and could not be activated in the absence of membranes (Fig. S1), consistent with efficient prenylation. We cannot rule out the possibility that the Rab substrates

are mono-prenylated rather than di-prenylated, but find it unlikely that mono-prenylation would significantly affect our interpretation of the data presented in this study.

Liposome preparation

Synthetic TGN liposomes were prepared using a mixture of lipids approximating the lipid composition of the TGN reported by a previous lipidomics study (Klemm et al., 2009). Lipids were combined, vacuum dried, and rehydrated in HK buffer (20 mM Hepes, pH 7.4, and 150 mM KOAc) by incubating overnight at 37°C. Lipids were then extruded though 100- or 400-nm filters (Whatman) to generate liposomes. 400-nm liposomes were used for pelleting assays; all other experiments were performed using 100-nm liposomes. Unless started otherwise, liposomes contain 5% Ni^{2+}-DOGS to anchor His-tagged Rabs. We found that the presence of Ni^{2+}-DOGS enabled TRAPPII to interact stably with TGN liposomes in the absence of Arf1-GTP. TGN liposomes lacking Ni^{2+}-DOGS required Arf1-GTP for stable membrane binding. This effect is not because of the presence of a His-tag (the purified TRAPPII complexes lacked His-tags) and rather appears to be a result of the positive charge of the Ni^{2+} ion, which may mimic some unknown factor in vivo. "TGN-anionic" and "TGN-neutral" liposomes contain only the anionic or neutral components of the TGN mix, respectively, with dioleoylphosphatidylcholine (DOPC) added to bring the final lipid concentration to 1 mM. Phosphatidylcholine (PC) liposomes contain 99% DOPC and 1% DiR (near-infrared dye). See Table S3 for the molar percentage of each lipid for the different liposomes used in this study.

GEF activity assays

GEF assays were performed under multiple-turnover conditions. Exchange of nonfluorescent GTP for mantGDP was measured by sequentially adding 333 µM liposomes, 200 µM nonfluorescent GTP, and 250 nM mantGDP-labeled Rab to HKM buffer at 30°C. This mixture was then incubated for 2 min before nucleotide exchange was initiated by the addition of TRAPP. Because of the faster exchange rate of His-tagged Rabs, 10 nM TRAPP was used for all reactions with Rab-His_7 substrates, whereas 13 nM TRAPP was used for all reactions with prenylated-Rab/GDI substrates. After the addition of TRAPP, mantGDP fluorescence was measured (365-nm excitation and 440-nm emission) for 20–30 min to obtain the exchange trace. For reactions with recruiter GTPases (Fig. 5 and Fig. S4), 1.5 µM recruiter GTPase was preactivated using EDTA-mediated exchange as previously described (McDonold and Fromme, 2014) before adding mantGDP-labeled Rab substrate and TRAPP. For competition assays (Fig. 2 and Fig. S2) mantGDP-labeled Rab and competing nonfluorescent Rab were premixed and added to the reaction simultaneously. All GEF assays were performed with $n \geq 3$, with the exception of reactions that exhibited no nucleotide exchange (for example, rTRAPPI-mediated Ypt31-His_7 activation), which were performed with $n \geq 2$ reactions. To determine exchange rates, curves of fluorescence versus time were fit to a single exponential curve with an additional linear drift term using Prism software (GraphPad Software). The resulting rate constants were divided by the concentration of GEF to give the exchange rate. In all figures, error bars represent 95% confidence intervals (CIs).

Without a bound GDI, His-tagged Rab substrates undergo intrinsic exchange in the presence of excess GTP. To control for the intrinsic exchange of His-tagged Rabs, mock reactions were performed with buffer added in lieu of TRAPP complexes. Rate constants were obtained for replicate mock reactions and averaged. Rates for TRAPP-catalyzed Rab-His_7 nucleotide exchange were calculated by subtracting the mean mock rate constant from that of the TRAPP-mediated exchange reaction before dividing by the GEF concentration.

Liposome flotation assays

To test GTPase and lipid recruitment of TRAPP complexes, 4–6 µg prenylated or myristoylated GTPase was mixed with 250 µM liposomes and 250 µM GMP-PNP or GDP in HK buffer. EDTA was added to a final concentration of 3 mM for 30 min at 30°C to mediate nucleotide exchange and drive membrane insertion of activated GTPases. The exchange reaction was stopped with the addition of 6 mM $MgCl_2$. 1 µg rTRAPP was then added, and the mixture was incubated at 30°C for 20 min. Membrane-associated proteins were separated from unbound proteins using discontinuous sucrose gradient flotation as previously described (Richardson and Fromme, 2015). Membrane-bound rTRAPP was detected via immunoblotting using the anti-TAP tag antibody for rTRAPPII (Trs130-TAP) and the anti-His_6 antibody for rTRAPPI (His_6-Trs31). Membrane-associated GTPases were visualized by staining total protein with BioSafe Coomassie (Bio-Rad Laboratories) or immunoblotting using the anti-Arf1 antibody.

Liposome pelleting assays

Liposome pelleting assays were performed to quantify the percentage of membrane-anchored His-tagged Rabs in GEF assays. 1 µg Rab-His_7 was mixed with 500 µM liposomes containing 5% Ni^{2+}-DOGS in HKM buffer and allowed to incubate at 30°C for 15 min. Membrane-associated protein was separated from unbound protein via liposome pelleting, and samples were analyzed as previously described (Paczkowski et al., 2012). Reactions lacking liposomes were run in parallel to control for background pelleting of His-tagged Rabs.

Liposome pelleting assays were also used to test whether Rabs were efficiently prenylated during the generation of Rab/GDI complexes. Prenylation reactions were performed with or without geranylgeranyl pyrophosphate (GGPP) to control for the possibility that Gdi1 may form low-affinity complexes with nonprenylated Rabs. Pooled fractions from both reactions were combined with 500 µM liposomes and 333 µM GTP or GDP. 3 mM EDTA was added, and the mixture was incubated at 30°C for 30 min to allow nucleotide exchange and membrane insertion of activated, prenylated-Rabs. The exchange reaction was stopped by the addition of 6 mM $MgCl_2$, and membrane-bound protein was isolated via liposome pelleting. Reactions lacking liposomes were run in parallel to control for background pelleting. As expected for prenylated Rabs, significant membrane binding was only observed with GTP-activated Rabs prepared with GGPP (see Fig. S1 C). A lesser amount of activated, prenylated Rab also pelleted in the absence of liposomes, likely because of aggregation from the hydrophobic prenyl groups that are exposed upon activation. We also note that all prenylated Rabs bind membranes after activation during liposome flotation assays (Fig. S4), consistent with efficient Rab prenylation.

Microscopy

Cells were grown in synthetic dropout media at 30°C unless otherwise noted and imaged in log-phase on glass coverslips or in glass-bottomed dishes. All images were processed using ImageJ, adjusting only the minimum/maximum brightness levels for clarity with equivalent processing of each image within an experimental panel. Each image shown is a single focal plane. Time-lapse series in Fig. 6 and S5 were generated by imaging every 2 s for 2–4 min, and peak-to-peak measurements were determined as previously described (McDonold and Fromme, 2014).

Images shown in Figs. 3, 4 (A and C), 5 (A and E), and S3 (A–D) were acquired using a DeltaVision RT wide-field deconvolution microscope (Applied Precision Ltd.), 100×/1.35 NA objective, and a CoolSNAP HQ camera (Photometrics). Images were captured and deconvolved using SoftWoRx software (Applied Precision Ltd.). All other imaging was performed using a CSU-X spinning disc confocal microscope system (Intelligent Imaging Innovations,

Inc.) using a DMI600B microscope (Leica Biosystems), 100×/1.46 NA objective, and a QuantEM EMCCD camera (Photometrics). Images were acquired using Slidebook 5.0 software (Intelligent Imaging Innovations, Inc.).

Image analysis

Pearson's analysis was used to quantify colocalization of fluorescently tagged proteins at Golgi compartments. Images were processed in ImageJ using the JACoP plugin to determine the Pearson's coefficient of colocalization. Recruitment of TRAPPII, Ypt31/32, or Arf2 to the late Golgi was measured by quantifying the ratio of TRAPPII-mNeonGreen, GFP-Ypt31/32, or GFP-Arf2 fluorescence to that of Sec7-RFP at Golgi compartments. Fluorescence ratios at individual Golgi compartments were quantified in ImageJ by first using Otsu autothresholding to convert Sec7-RFP punctae into regions of interest and then using the Multimeasure tool to quantify fluorescence in each region of interest. Line-trace analysis to quantify the amount of cytosolic versus Golgi-localized TRAPPII was performed using ImageJ as previously described (Richardson et al., 2012).

Statistical tests

For Figs. 1 D, 2 C, 4, 5 C, S2 C, S3, and S4 A, statistical significance was determined using an unpaired *t* test with Welch's correction. For all other figures, significance was determined using a one-way analysis of variance with Tukey's test for multiple comparison.

Online supplemental material

Fig. S1 describes the workflow used to generate prenylated-Rab/GDI complexes and shows GEF activity assay controls. Fig. S2 demonstrates that TRAPP catalytic site mutants do not affect complex assembly. Fig. S3 shows controls for in vivo experiments using TRAPPII mutants and the Sec7 inhibitor MNTC. Fig. S4 shows controls for TRAPPII membrane-recruitment assays. Fig. S5 shows that TRAPPII localizes primarily to the late Golgi and colocalizes with Ypt1 in *gyp1Δ* cells. Tables S1 and S2 describe the plasmids and strains used in this study, respectively. Table S3 lists the lipid composition of each type of liposome used in this study.

Acknowledgments

We thank the laboratories of A. Bretscher, R. Collins, S. Emr, S. Ferro-Novick, B. Glick, T. Graham, L. Miller, H. Pelham, K. Reinisch, R. Schekman, N. Segev, and C. Ungermann for generously sharing reagents, strains, plasmids, equipment, and advice. We are grateful to C. Ungermann, L. Langemeyer, and X. Shu for advice and assistance in generating prenylated-Rab/GDI complexes and S. Emr, A. Bretscher, L. Miller, and B. Richardson for helpful discussions and feedback.

This work was funded by National Institutes of Health grants R01GM098621 and R01GM116942 and training grant T32GM007273.

The authors declare no competing financial interests.

Author contributions: L.L. Thomas designed and conducted the experiments and wrote the manuscript. J.C. Fromme conceived the project and assisted with writing the manuscript.

Submitted: 31 August 2016
Revised: 7 October 2016
Accepted: 14 October 2016

References

Barr, F.A. 2009. Rab GTPase function in Golgi trafficking. *Semin. Cell Dev. Biol.* 20:780–783. http://dx.doi.org/10.1016/j.semcdb.2009.03.007

Barrowman, J., D. Bhandari, K. Reinisch, and S. Ferro-Novick. 2010. TRAPP complexes in membrane traffic: convergence through a common Rab. *Nat. Rev. Mol. Cell Biol.* 11:759–763. http://dx.doi.org/10.1038/nrm2999

Benli, M., F. Döring, D.G. Robinson, X. Yang, and D. Gallwitz. 1996. Two GTPase isoforms, Ypt31p and Ypt32p, are essential for Golgi function in yeast. *EMBO J.* 15:6460–6475.

Bigay, J., and B. Antonny. 2012. Curvature, lipid packing, and electrostatics of membrane organelles: Defining cellular territories in determining specificity. *Dev. Cell.* 23:886–895. http://dx.doi.org/10.1016/j.devcel.2012.10.009

Brunet, S., and M. Sacher. 2014. In sickness and in health: The role of TRAPP and associated proteins in disease. *Traffic.* 15:803–818. http://dx.doi.org/10.1111/tra.12183

Cabrera, M., M. Nordmann, A. Perz, D. Schmedt, A. Gerondopoulos, F. Barr, J. Piehler, S. Engelbrecht-Vandré, and C. Ungermann. 2014. The Mon1-Ccz1 GEF activates the Rab7 GTPase Ypt7 via a longin-fold-Rab interface and association with PI3P-positive membranes. *J. Cell Sci.* 127:1043–1051. http://dx.doi.org/10.1242/jcs.140921

Cai, H., K. Reinisch, and S. Ferro-Novick. 2007. Coats, tethers, Rabs, and SNAREs work together to mediate the intracellular destination of a transport vesicle. *Dev. Cell.* 12:671–682. http://dx.doi.org/10.1016/j.devcel.2007.04.005

Cai, Y., H.F. Chin, D. Lazarova, S. Menon, C. Fu, H. Cai, A. Sclafani, D.W. Rodgers, E.M. De La Cruz, S. Ferro-Novick, and K.M. Reinisch. 2008. The structural basis for activation of the Rab Ypt1p by the TRAPP membrane-tethering complexes. *Cell.* 133:1202–1213. http://dx.doi.org/10.1016/j.cell.2008.04.049

Chen, C.Y., and T.R. Graham. 1998. An arf1Δ synthetic lethal screen identifies a new clathrin heavy chain conditional allele that perturbs vacuolar protein transport in *Saccharomyces cerevisiae*. *Genetics.* 150:577–589.

Chen, S., H. Cai, S.K. Park, S. Menon, C.L. Jackson, and S. Ferro-Novick. 2011. Trs65p, a subunit of the Ypt1p GEF TRAPPII, interacts with the Arf1p exchange factor Gea2p to facilitate COPI-mediated vesicle traffic. *Mol. Biol. Cell.* 22:3634–3644. http://dx.doi.org/10.1091/mbc.E11-03-0197

D'Angelo, G., M. Vicinanza, A. Di Campli, and M.A. De Matteis. 2008. The multiple roles of PtdIns(4)P -- not just the precursor of PtdIns(4,5)P2. *J. Cell Sci.* 121:1955–1963. http://dx.doi.org/10.1242/jcs.023630

Daboussi, L., G. Costaguta, and G.S. Payne. 2012. Phosphoinositide-mediated clathrin adaptor progression at the trans-Golgi network. *Nat. Cell Biol.* 14:239–248. http://dx.doi.org/10.1038/ncb2427

De Matteis, M.A., and A. Luini. 2008. Exiting the Golgi complex. *Nat. Rev. Mol. Cell Biol.* 9:273–284. http://dx.doi.org/10.1038/nrm2378

DiNitto, J.P., A. Delprato, M.T. Gabe Lee, T.C. Cronin, S. Huang, A. Guilherme, M.P. Czech, and D.G. Lambright. 2007. Structural basis and mechanism of autoregulation in 3-phosphoinositide-dependent Grp1 family Arf GTPase exchange factors. *Mol. Cell.* 28:569–583. http://dx.doi.org/10.1016/j.molcel.2007.09.017

Feng, Q., D. Baird, and R.A. Cerione. 2004. Novel regulatory mechanisms for the Dbl family guanine nucleotide exchange factor Cool-2/alpha-Pix. *EMBO J.* 23:3492–3504. http://dx.doi.org/10.1038/sj.emboj.7600331

Gillingham, A.K., R. Sinka, I.L. Torres, K.S. Lilley, and S. Munro. 2014. Toward a comprehensive map of the effectors of rab GTPases. *Dev. Cell.* 31:358–373. http://dx.doi.org/10.1016/j.devcel.2014.10.007

Glick, B.S., and A. Nakano. 2009. Membrane traffic within the Golgi apparatus. *Annu. Rev. Cell Dev. Biol.* 25:113–132. http://dx.doi.org/10.1146/annurev.cellbio.24.110707.175421

Goody, R.S., A. Rak, and K. Alexandrov. 2005. The structural and mechanistic basis for recycling of Rab proteins between membrane compartments. *Cell. Mol. Life Sci.* 62:1657–1670. http://dx.doi.org/10.1007/s00018-005-4486-8

Hankins, H.M., Y.Y. Sere, N.S. Diab, A.K. Menon, and T.R. Graham. 2015. Phosphatidylserine translocation at the yeast trans-Golgi network regulates protein sorting into exocytic vesicles. *Mol. Biol. Cell.* 26:4674–4685. http://dx.doi.org/10.1091/mbc.E15-07-0487

Itzen, A., A. Rak, and R.S. Goody. 2007. Sec2 is a highly efficient exchange factor for the Rab protein Sec4. *J. Mol. Biol.* 365:1359–1367. http://dx.doi.org/10.1016/j.jmb.2006.10.096

Jackson, C.L., and S. Bouvet. 2014. Arfs at a glance. *J. Cell Sci.* 127:4103–4109. http://dx.doi.org/10.1242/jcs.144899

Jedd, G., C. Richardson, R. Litt, and N. Segev. 1995. The Ypt1 GTPase is essential for the first two steps of the yeast secretory pathway. *J. Cell Biol.* 131:583–590. http://dx.doi.org/10.1083/jcb.131.3.583

Jedd, G., J. Mulholland, and N. Segev. 1997. Two new Ypt GTPases are required for exit from the yeast trans-Golgi compartment. *J. Cell Biol.* 137:563–580. http://dx.doi.org/10.1083/jcb.137.3.563

Jian, X., M. Cavenagh, J.M. Gruschus, P. Randazzo, and R. Kahn. 2011. Modifications to the C-terminus of Arf1 alter cell functions and protein interactions. *Traffic.* 11:732–742. http://dx.doi.org/10.1111/j.1600-0854.2010.01054.x

Jones, S., C. Newman, F. Liu, and N. Segev. 2000. The TRAPP complex is a nucleotide exchanger for Ypt1 and Ypt31/32. *Mol. Biol. Cell.* 11:4403–4411. http://dx.doi.org/10.1091/mbc.11.12.4403

Kim, J.J., Z. Lipatova, U. Majumdar, and N. Segev. 2016. Regulation of Golgi cisternal progression by Ypt/Rab GTPases. *Dev. Cell.* 36:440–452. http://dx.doi.org/10.1016/j.devcel.2016.01.016

Kim, Y.G., E.J. Sohn, J. Seo, K.J. Lee, H.S. Lee, I. Hwang, M. Whiteway, M. Sacher, and B.H. Oh. 2005. Crystal structure of bet3 reveals a novel mechanism for Golgi localization of tethering factor TRAPP. *Nat. Struct. Mol. Biol.* 12:38–45. http://dx.doi.org/10.1038/nsmb871

Klemm, R.W., C.S. Ejsing, M.A. Surma, H.J. Kaiser, M.J. Gerl, J.L. Sampaio, Q. de Robillard, C. Ferguson, T.J. Proszynski, A. Shevchenko, and K. Simons. 2009. Segregation of sphingolipids and sterols during formation of secretory vesicles at the trans-Golgi network. *J. Cell Biol.* 185:601–612. http://dx.doi.org/10.1083/jcb.200901145

Lee, A.Y., R.P. St Onge, M.J. Proctor, I.M. Wallace, A.H. Nile, P.A. Spagnuolo, Y. Jitkova, M. Gronda, Y. Wu, M.K. Kim, et al. 2014. Mapping the cellular response to small molecules using chemogenomic fitness signatures. *Science.* 344:208–211. http://dx.doi.org/10.1126/science.1250217

Lynch-Day, M.A., D. Bhandari, S. Menon, J. Huang, H. Cai, C.R. Bartholomew, J.H. Brumell, S. Ferro-Novick, and D.J. Klionsky. 2010. Trs85 directs a Ypt1 GEF, TRAPPIII, to the phagophore to promote autophagy. *Proc. Natl. Acad. Sci. USA.* 107:7811–7816. http://dx.doi.org/10.1073/pnas.1000063107

McDonold, C.M., and J.C. Fromme. 2014. Four GTPases differentially regulate the Sec7 Arf-GEF to direct traffic at the trans-golgi network. *Dev. Cell.* 30:759–767. http://dx.doi.org/10.1016/j.devcel.2014.07.016

Mizuno-Yamasaki, E., M. Medkova, J. Coleman, and P. Novick. 2010. Phosphatidylinositol 4-phosphate controls both membrane recruitment and a regulatory switch of the Rab GEF Sec2p. *Dev. Cell.* 18:828–840. http://dx.doi.org/10.1016/j.devcel.2010.03.016

Morozova, N., Y. Liang, A.A. Tokarev, S.H. Chen, R. Cox, J. Andrejic, Z. Lipatova, V.A. Sciorra, S.D. Emr, and N. Segev. 2006. TRAPPII subunits are required for the specificity switch of a Ypt-Rab GEF. *Nat. Cell Biol.* 8:1263–1269. http://dx.doi.org/10.1038/ncb1489

Novick, P. 2016. Regulation of membrane traffic by Rab GEF and GAP cascades. *Small GTPases*. 1–5. http://dx.doi.org/10.1080/21541248.2016.1213781

Paczkowski, J.E., B.C. Richardson, A.M. Strassner, and J.C. Fromme. 2012. The exomer cargo adaptor structure reveals a novel GTPase-binding domain. *EMBO J.* 31:4191–4203. http://dx.doi.org/10.1038/emboj.2012.268

Papanikou, E., and B.S. Glick. 2014. Golgi compartmentation and identity. *Curr. Opin. Cell Biol.* 29:74–81. http://dx.doi.org/10.1016/j.ceb.2014.04.010

Pfeffer, S.R. 2012. Rab GTPase localization and Rab cascades in Golgi transport. *Biochem. Soc. Trans.* 40:1373–1377. http://dx.doi.org/10.1042/BST20120168

Pinar, M., H.N. Arst Jr., A. Pantazopoulou, V.G. Tagua, V. de los Ríos, J. Rodríguez-Salarichs, J.F. Díaz, and M.A. Peñalva. 2015. TRAPPII regulates exocytic Golgi exit by mediating nucleotide exchange on the Ypt31 ortholog RabERAB11. *Proc. Natl. Acad. Sci. USA.* 112:4346–4351. http://dx.doi.org/10.1073/pnas.1419168112

Qi, X., M. Kaneda, J. Chen, A. Geitmann, and H. Zheng. 2011. A specific role for *Arabidopsis* TRAPPII in post-Golgi trafficking that is crucial for cytokinesis and cell polarity. *Plant J.* 68:234–248. http://dx.doi.org/10.1111/j.1365-313X.2011.04681.x

Richardson, B.C., and J.C. Fromme. 2015. Biochemical methods for studying kinetic regulation of Arf1 activation by Sec7. *Methods Cell Biol.* 130:101–126. http://dx.doi.org/10.1016/bs.mcb.2015.03.020

Richardson, B.C., C.M. McDonold, and J.C. Fromme. 2012. The Sec7 Arf-GEF is recruited to the trans-Golgi network by positive feedback. *Dev. Cell.* 22:799–810. http://dx.doi.org/10.1016/j.devcel.2012.02.006

Rivera-Molina, F.E., and P.J. Novick. 2009. A Rab GAP cascade defines the boundary between two Rab GTPases on the secretory pathway. *Proc. Natl. Acad. Sci. USA.* 106:14408–14413. http://dx.doi.org/10.1073/pnas.0906536106

Robinett, C.C., M.G. Giansanti, M. Gatti, and M.T. Fuller. 2009. TRAPPII is required for cleavage furrow ingression and localization of Rab11 in dividing male meiotic cells of *Drosophila*. *J. Cell Sci.* 122:4526–4534. http://dx.doi.org/10.1242/jcs.054536

Sacher, M., Y.-G. Kim, A. Lavie, B.-H. Oh, and N. Segev. 2008. The TRAPP complex: Insights into its architecture and function. *Traffic.* 9:2032–2042. http://dx.doi.org/10.1111/j.1600-0854.2008.00833.x

Santiago-Tirado, F.H., A. Legesse-Miller, D. Schott, and A. Bretscher. 2011. PI4P and Rab inputs collaborate in myosin-V-dependent transport of secretory compartments in yeast. *Dev. Cell.* 20:47–59. http://dx.doi.org/10.1016/j.devcel.2010.11.006

Sciorra, V.A., A. Audhya, A.B. Parsons, N. Segev, C. Boone, and S.D. Emr. 2005. Synthetic genetic array analysis of the PtdIns 4-kinase Pik1p identifies components in a Golgi-specific Ypt31/rab-GTPase signaling pathway. *Mol. Biol. Cell.* 16:776–793. http://dx.doi.org/10.1091/mbc.E04-08-0700

Sclafani, A., S. Chen, F. Rivera-Molina, K. Reinisch, P. Novick, and S. Ferro-Novick. 2010. Establishing a role for the GTPase Ypt1p at the late Golgi. *Traffic.* 11:520–532. http://dx.doi.org/10.1111/j.1600-0854.2010.01031.x

Segev, N. 2001. Ypt/rab gtpases: regulators of protein trafficking. *Sci. STKE.* 2001:re11.

Sondermann, H., S.M. Soisson, S. Boykevisch, S.S. Yang, D. Bar-Sagi, and J. Kuriyan. 2004. Structural analysis of autoinhibition in the Ras activator Son of sevenless. *Cell.* 119:393–405. http://dx.doi.org/10.1016/j.cell.2004.10.005

Stalder, D., and B. Antonny. 2013. Arf GTPase regulation through cascade mechanisms and positive feedback loops. *FEBS Lett.* 587:2028–2035. http://dx.doi.org/10.1016/j.febslet.2013.05.015

van Meer, G., D.R. Voelker, and G.W. Feigenson. 2008. Membrane lipids: Where they are and how they behave. *Nat. Rev. Mol. Cell Biol.* 9:112–124. http://dx.doi.org/10.1038/nrm2330

Wang, W., and S. Ferro-Novick. 2002. A Ypt32p exchange factor is a putative effector of Ypt1p. *Mol. Biol. Cell.* 13:3336–3343. http://dx.doi.org/10.1091/mbc.01-12-0577

Wang, W., M. Sacher, and S. Ferro-Novick. 2000. TRAPP stimulates guanine nucleotide exchange on Ypt1p. *J. Cell Biol.* 151:289–296. http://dx.doi.org/10.1083/jcb.151.2.289

Westlake, C.J., L.M. Baye, M.V. Nachury, K.J. Wright, K.E. Ervin, L. Phu, C. Chalouni, J.S. Beck, D.S. Kirkpatrick, D.C. Slusarski, et al. 2011. Primary cilia membrane assembly is initiated by Rab11 and transport protein particle II (TRAPPII) complex-dependent trafficking of Rabin8 to the centrosome. *Proc. Natl. Acad. Sci. USA.* 108:2759–2764. http://dx.doi.org/10.1073/pnas.1018823108

Xu, P., R.D. Baldridge, R.J. Chi, C.G. Burd, and T.R. Graham. 2013. Phosphatidylserine flipping enhances membrane curvature and negative charge required for vesicular transport. *J. Cell Biol.* 202:875–886. http://dx.doi.org/10.1083/jcb.201305094

Yamamoto, K., and Y. Jigami. 2002. Mutation of TRS130, which encodes a component of the TRAPP II complex, activates transcription of OCH1 in *Saccharomyces cerevisiae*. *Curr. Genet.* 42:85–93. http://dx.doi.org/10.1007/s00294-002-0336-5

Yip, C.K., J. Berscheminski, and T. Walz. 2010. Molecular architecture of the TRAPPII complex and implications for vesicle tethering. *Nat. Struct. Mol. Biol.* 17:1298–1304. http://dx.doi.org/10.1038/nsmb.1914

Zhang, C.J., J.B. Bowzard, M. Greene, A. Anido, K. Stearns, and R.A. Kahn. 2002. Genetic interactions link ARF1, YPT31/32 and TRS130. *Yeast.* 19:1075–1086. http://dx.doi.org/10.1002/yea.903

Zou, S., Y. Liu, X.Q. Zhang, Y. Chen, M. Ye, X. Zhu, S. Yang, Z. Lipatova, Y. Liang, and N. Segev. 2012. Modular TRAPP complexes regulate intracellular protein trafficking through multiple Ypt/Rab GTPases in *Saccharomyces cerevisiae*. *Genetics.* 191:451–460. http://dx.doi.org/10.1534/genetics.112.139378